J. Math. Biol. 48, 243–274 (2004)
Digital Object Identifier (DOI):
10.1007/s00285-003-0228-4

Mathematical Biology

Remus Oşan · Rodica Curtu · Jonathan Rubin · Bard Ermentrout

Multiple-spike waves in a one-dimensional integrate-and-fire neural network

Received: 7 August 2002 / Revised version: 15 April 2003 /
Published online: 20 August 2003 –

Abstract. This paper builds on the past study of single-spike waves in one-dimensional integrate-and-fire networks to provide a framework for the study of waves with arbitrary (finite or countably infinite) collections of spike times. Based on this framework, we prove an existence theorem for single-spike traveling waves, and we combine analysis and numerics to study two-spike traveling waves, periodic traveling waves, and general infinite spike trains. For a fixed wave speed, finite-spike waves, periodic waves, and other infinite-spike waves may all occur, and we discuss the relationships among them. We also relate the waves considered analytically to waves generated in numerical simulations by the transient application of localized excitation.

1. Introduction

Traveling waves in networks of neurons with purely excitatory synaptic coupling have been the object of many recent theoretical studies [2,3,7,8,10,11,14–18]. These studies are motivated by experiments in which a slice of cortical tissue, with all inhibition blocked, is subjected to a local shock stimulus. This stimulus results in a wave of activity propagating across the network [4,5,9,13,22]. Theoretical models of this phenomenon range from continuum firing rate models [1,18] to simplified spiking models [2,7,17] to detailed conductance-based models [9,22].

Firing rate models do not include individual spikes; as a result, the temporal details of neuronal activity cannot be considered. In spiking models (and in experiments), it becomes apparent that after the first wave front passes through a network, a single neuron can fire many times [9,19]. However, theoretical analysis of spiking models has, with few exceptions, required that *each neuron fire exactly once* during wave propagation. This is either *a priori* imposed on the model or implemented by strong synaptic depression or after-hyperpolarization. In the single-spike case, the existence of traveling waves is reduced to solving a certain nonautonomous boundary value problem [7,17]. This computation can be done explicitly when the individual neurons are modeled by the leaky integrate-and-fire (LIF) model. Ermentrout [7], Bressloff [2] and Golomb and Ermentrout [10,11] developed

R. Oşan, R. Curtu, J. Rubin*, B. Ermentrout: Department of Mathematics, University of Pittsburgh, Pittsburgh, PA 15260 USA.

*Corresponding author: e-mail: rubin@math.pitt.edu

Key words or phrases: Traveling waves – Integrate-and-fire network – Excitatory synaptic coupling

methods for studying the existence of traveling waves of activity in networks of LIF cells, incorporating a variety of additional features such as synaptic delays, again under the assumption that each cell only fires once. Under this assumption it is also possible to obtain an expression for the wave velocity c [16].

In this paper, we aim to address several questions related to networks of spiking neurons in which *each cell fires multiple spikes* during wave propagation. As with most previous analysis, we will restrict our attention to an excitatorily coupled network of LIF neurons. Recall that the LIF model for an individual neuron has the form

$$\tau_1 \frac{dV}{dt} = -V + I(t)\,,$$

where $I(t)$ represents inputs and τ_1 is the membrane time constant. If $V(t^-) = V_T$, the voltage threshold, then $V(t^+) = V_R$, the reset voltage, and the neuron emits a "spike." We can formally rewrite this equation to take into account the resetting as

$$\tau_1 \frac{dV}{dt} = -V + I(t) + \tilde{V}_R \sum_n \delta(t - t_n) \tag{1}$$

where $\tilde{V}_R = \tau_1(V_R - V_T)$ and t_n denotes the sequence of firing times of the neuron; that is, $V(t_n^-) = V_T$ for each $n \geq 1$. Henceforth, we omit the $-$ (minus) superscript when taking the limit of V as t approaches a firing time from the left.

We consider a continuous network of such neurons, coupled in a translationally invariant manner on an infinite one-dimensional domain and parameterized by the spatial variable, x. The model is identical to those studied in many of the papers mentioned above. Coupling between a neuron at position x and one at position y is mediated by a time-dependent current with maximal strength depending on the distance, $|x - y|$. Each time a neuron fires, it activates a potential defined by a fixed function, $\alpha(t)$, which vanishes for $t < 0$, is typically positive for $t > 0$, and decays to zero as $t > 0$ increases. With these considerations, the network of interest is:

$$\begin{aligned}\tau_1 \frac{\partial V}{\partial t} = -V(x,t) + g \sum_{n=-\infty}^{\infty} \int_{-\infty}^{\infty} dy\, J(x-y)\, \alpha(t - t_n^*(y)) \\ + \sum_{n=-\infty}^{\infty} \delta(t - t_n^*(x))\, \tilde{V}_R\end{aligned} \tag{2}$$

for $(x,t) \in \mathbb{R} \times \mathbb{R}$, where $\tilde{V}_R$ is given in (1); we assume that $V_R < V_T$. In this continuous network, note that the firing times $t_n^*(x)$ have a spatial dependence. Integration of (2) yields $V(x, t_n^*(x)) = V_T$ and $V(x, t_n^{*+}(x)) = V_R$, which verifies that the constant $\tilde{V}_R$ is defined appropriately.

In (2), the parameter g denotes maximal synaptic coupling strength, while $J(x) : \mathbb{R} \to \mathbb{R}^+ \cup \{0\}$ is the synaptic coupling function, with integral 1. Any integrable, even, non-negative function could be used here. In this paper, we take

$$\alpha(t) = e^{-t/\tau_2} H(t) = \begin{cases} 0, & t < 0 \\ e^{-t/\tau_2}, & t \geq 0 \end{cases} \tag{3}$$

where $H(t)$ is the Heaviside step function, $\tau_1 < \tau_2$ and

$$J(x) = \frac{1}{2\sigma} e^{-|x|/\sigma} . \tag{4}$$

Our results will extend to any qualitatively similar pair of functions; however, these specific choices allow us to make explicit calculations which would become unwieldy in more general cases. Other examples are discussed in [14].

Numerical simulations indicate that the type of neural network given in (2) can support a great variety of constant speed traveling wave solutions in which each cell fires multiple spikes. Figure 1 shows an example of traveling waves emanating from a transient localized stimulus. Bressloff [3] derives a dispersion relation between wave speed c and wave number k in the special case of periodic traveling waves, with $t_n^*(x) = (kx + n)T$ for each integer n and $c = (kT)^{-1}$. He also characterizes how this relation depends on rise-time of synaptic coupling, synaptic delays, and dendritic cable properties. In this paper, we provide a framework for the study of traveling waves with arbitrary (finite or countably infinite) collections of spike times. We first, in Section 2, provide a reformulation of (2) which is particularly suitable for the study of traveling waves. In Section 3, we use this to provide a necessary and sufficient condition for the existence of single-spike traveling waves, thereby completing the partial study of such waves begun in [2,7], and to analyze two-spike traveling waves.

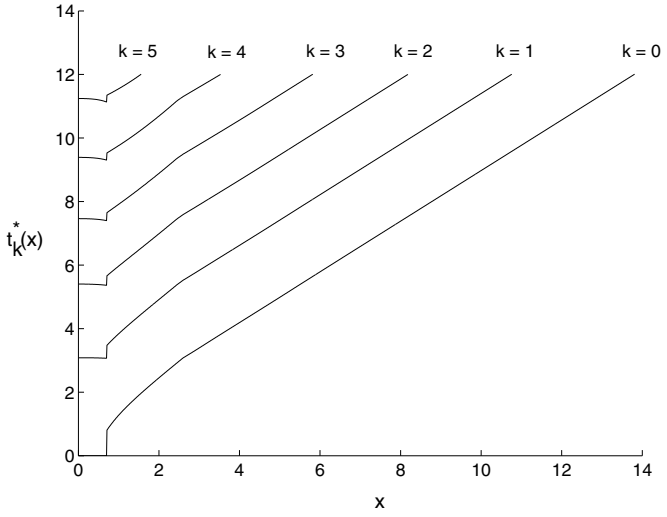

Fig. 1. Numerically simulated traveling waves. Time increases along the vertical axis, while space increases along the horizontal axis. The curves shown indicate the times and positions at which spikes occur. At the start of the simulation, all cells are at rest, and cells in the leftmost region shown are given a transient excitatory input. No further inputs are given; all subsequent waves emerge spontaneously. The simulation is performed on a spatial region that is symmetric about $x = 0$; symmetric waves propagate out to the left (negative x) in the simulation but are not shown here.

Ermentrout [7] showed that for fixed parameters, wave speed depends only weakly on the number of spikes fired by each cell in an integrate-and-fire network. Oşan and Ermentrout [15] showed similar results for a network of theta neurons (another simple one-variable model for neurons). In numerical computations, wave propagation can be initiated by application of a transient excitatory stimulus at a fixed time and location. In these simulations, as waves propagate through the network, it appears that the interspike intervals for cells with large x become independent of x. We analytically calculate the interspike interval for a two-spike wave here, and our results yield an excellent agreement with the interspike interval at large x for multiple-spike waves simulated numerically.

Moving beyond finite-spike solutions, in Section 4 we consider traveling wave solutions for which each cell spikes at an infinite sequence $\{T_n(x)\}$, $n \geq 0$, of spike times. Our traveling wave formulation can be used naturally for the iterative computation of the interspike intervals $T_{n+1} - T_n$ that must arise for such a solution to be consistent with equations (2), (3), (4). Next, we analyze periodic solutions, deriving a three-branched dispersion relation between wave speed c and period T. Finally, we give some indications that in certain parameter regimes, the interspike intervals of infinite-spike traveling waves with speed c monotonically decrease towards the period T for the periodic solution with the same speed, as $n \to \infty$.

2. Traveling wave description

We begin by considering constant speed traveling wave solutions of (2) for which each cell has a finite first spike time. That is, we exclude periodic solutions, which we discuss in Section 4.2. For non-periodic solutions, the n-th spike time, $n \geq 0$, of the neuron at the position x can be written as $t_n^*(x) = \frac{x}{c} + T_n$. Here we assume $T_0 = 0$, and $\{T_n\}_{n\geq 0}$ is a sequence of nonnegative numbers $T_0 = 0 < T_1 \leq \ldots \leq T_N \leq \ldots$, with strict inequality as long as the T_n are finite. Traveling wave solutions of (2) take the form $V(x,t) = V(\xi)$ for traveling wave coordinate $\xi = tc - x \in \mathbb{R}$, where c denotes the traveling wave velocity. In terms of this coordinate, and under the assumption that each cell's first spike occurs at a finite time, equation (2) becomes

$$\tau_1 c\, V'(\xi) = -V(\xi) + g \sum_{n=0}^{\infty} \int_{-\infty}^{\infty} du\, J(u-\xi)\alpha(u/c - T_n) + \sum_{n=0}^{\infty} \delta(\xi/c - T_n)\tilde{V}_R. \tag{5}$$

A traveling wave solution of (5) is obtained by direct integration. For such a solution to be valid, it must satisfy a self-consistency condition, which we state here. This consistency condition relates the asymptotic behavior of V as $\xi \to -\infty$ with the fact that V reaches threshold for the first time at $\xi = 0$. In the limit as $\xi \to -\infty$, the synaptic input to each cell becomes 0 (that is, all wave fronts become infinitely far away from each cell). Since solutions of the equation $\tau_1 c V'(\xi) = -V(\xi)$ decay to 0, the consistency condition states that the potential of each neuron must satisfy $\lim_{\xi\to-\infty} V(\xi) = 0$. Upon integration of (5) from $\xi = -\infty$ to $\xi = 0$, using

$V(0) = V_T$, this condition formally yields

$$V_T = \frac{g\left(\sum_{n=0}^{\infty} e^{-\frac{c\,T_n}{\sigma}}\right)}{2\left(\frac{\tau_1 c}{\sigma}+1\right)\left(1+\frac{\sigma}{\tau_2 c}\right)}. \tag{6}$$

The derivation of the consistency condition (6) will become more clear in subsection 2.2.

For expression (6) to be meaningful, a second condition must hold, namely that the series $\sum_{n=0}^{\infty} e^{-c\,T_n/\sigma}$ is convergent; we will only consider traveling wave solutions for which this is true. Clearly this holds if each neuron fires only a finite number M of times. In this case, we obtain $T_0 = 0 < T_1 < \ldots < T_{M-1} < \infty$ and set $T_n = \infty$ for all $n \geq M$; thus, the series becomes the finite sum $\sum_{n=0}^{\infty} e^{-c\,T_n/\sigma} = \sum_{n=0}^{M-1} e^{-c\,T_n/\sigma}$.

Using the consistency condition (6), integration of (5) up to arbitrary ξ yields

$$V(\xi) = V_T\, e^{-\xi/\tau_1 c} + I_{syn}(\xi) + R(\xi). \tag{7}$$

The function $R(\xi)$ is the "decaying reset," encoding the refractoriness of a cell after a spike. This is given by $R(\xi) = \sum_{n=0}^{\infty} \eta(\xi/c - T_n)$ where

$$\eta(t) = \begin{cases} 0 & , \quad t \leq 0 \\ (V_R - V_T)\, e^{-t/\tau_1} & , \quad t > 0 \end{cases} \tag{8}$$

and $I_{syn}(\xi)$ is the "synaptic integral"

$$\begin{aligned} I_{syn}(\xi) &= \frac{g}{\tau_1 c}\, e^{-\xi/\tau_1 c} \int_0^{\xi} ds \left[\sum_{n=0}^{\infty} \int_0^{\infty} du\, J(u + c\,T_n - s)\alpha(u/c)\right] e^{s/\tau_1 c} \\ &\equiv (e^{-\xi/\tau_1 c}/\tau_1 c) \int_0^{\xi} ds \left(\sum_{n=0}^{\infty} I_n(s)\right) e^{s/\tau_1 c}. \end{aligned} \tag{9}$$

On each interval between two consecutive spikes the decaying reset has the form

$$R(\xi) = \begin{cases} 0 & , \quad \xi \leq 0 \\ (V_R - V_T)\left(\sum_{n=0}^{N-1} e^{T_n/\tau_1}\right) e^{-\xi/\tau_1 c} & , \quad c\,T_{N-1} < \xi \leq c\,T_N \ (N \geq 1). \end{cases}$$

The balance between the input from the synaptic integral and the reset after spiking determines what types of constant speed wave fronts can propagate in the neural network.

2.1. Computation of synaptic currents

We now derive the synaptic current due to the n-th front of the traveling wave, $I_n(s) = g\int_0^\infty du\, J(u + c\,T_n - s)\alpha(u/c)$, at some point s on the traveling wave coordinate axis.

Suppose we freeze the time t and record what happens at each position in space along the neural network. Without loss of generality, we fix our point of reference at $x = 0$, where by assumption the first spike occurs at $t = 0$ (such that $\xi = ct - x = 0$).

For any fixed negative time t, none of the wave fronts has yet reached the point $x = 0$, and all synaptic current results from waves that will arrive in the future. The n-th front ($n \geq 0$) will reach $x = 0$ at time T_n. Hence, one can derive the position y_n of the n-th front at time $t < T_n$ from $0 - y_n = c(T_n - t)$, which gives $y_n = c(t - T_n) < 0$. Correspondingly, the current (measured at $x = 0$) that is induced by this front ("future wave") at time t is

$$I_{n;\,f}(t) = g\int_{-\infty}^{c(t-T_n)} dy\, J(y)\,\alpha(t - y/c - T_n)\,.$$

Written in the wave coordinates ($s = ct - x = ct$, $u = ct - y - cT_n = s - y - cT_n$), and using the fact that J is an even function and that $u + cT_n - s = -y > 0$, this becomes

$$\begin{aligned} I_n(s) \equiv I_{n;\,f}(s) &= g\int_0^\infty du\, J(u + cT_n - s)\,\alpha(u/c) \\ &= \frac{g}{2\sigma}\int_0^\infty du\, e^{-(u+cT_n-s)/\sigma} e^{-u/\tau_2 c} = \frac{g\, e^{-cT_n/\sigma}}{2(1 + \frac{\sigma}{\tau_2 c})}\, e^{s/\sigma}\,. \end{aligned}$$

In summary, for t (and thus s) negative, all the synaptic currents correspond to "future waves" ($I_{n;\,f}$) and the total current at s is

$$I_{total}(s) = \sum_{n=0}^{\infty} I_n(s) = \frac{g\,\left(\sum_{n=0}^{\infty} e^{-cT_n/\sigma}\right)}{2(1 + \frac{\sigma}{\tau_2 c})}\, e^{s/\sigma}\,. \tag{10}$$

At any fixed nonnegative time t (such that $s = ct \geq 0$), say between two consecutive spike-times $T_{N-1} < t \leq T_N$, there are "previous wave" fronts that have already passed through $x = 0$ and many others that have yet to arrive. The position reached by each front at the moment t can be found by the same formula, $y_n = c(t - T_n)$, as above; the only difference is that $y_n > 0$ for all previous waves ($n = 0, \ldots, N - 1$) and $y_n \leq 0$ for all "future waves" ($n \geq N$). This classification of waves is illustrated in Figure 2. The synaptic currents are characterized below:

Synaptic current due to a future wave ($\mathbf{n \geq N}$)

$$\begin{aligned} I_n(s) = I_{n;\,f}(s) &= g\int_{-\infty}^{c(t-T_n)} dy\, J(y)\,\alpha(t - y/c - T_n) \\ &= g\int_0^\infty du\, J(u + cT_n - s)\,\alpha(u/c) = \frac{g\, e^{-cT_n/\sigma}}{2(1 + \frac{\sigma}{\tau_2 c})}\, e^{s/\sigma}\,. \end{aligned}$$

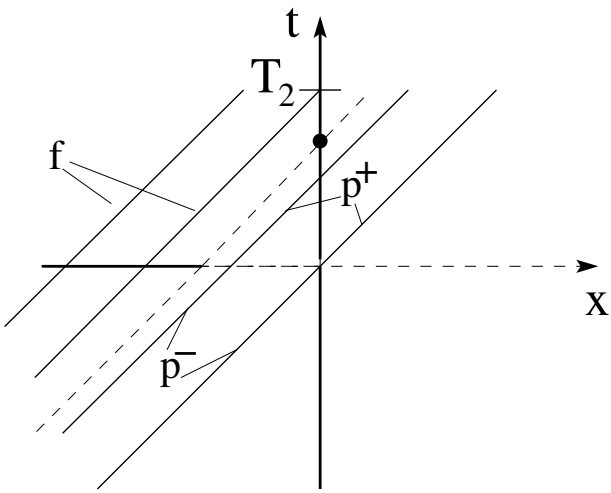

Fig. 2. Illustration of incoming waves relative to the cell at $x = 0$ at the time labelled with the solid black circle on the t-axis. At that time, the two waves labelled with 'f' are future waves for this cell, as they have not yet reached $x = 0$; one of them will arrive at time T_2 and the other at time T_3 (not shown). The two waves to the right of the diagonal dashed line are previous waves, as they have already passed through $x = 0$. We subdivide the synaptic contribution from these waves into p^- and p^+, below and above the horizontal dashed line, respectively; these correspond to synaptic inputs from spikes that occurred for some $t < 0$ and from spikes that occurred for some time $t > 0$, respectively.

Synaptic current due to a previous wave ($\mathbf{n = 0, \ldots, N - 1}$)

$$I_n(s) = I_{n;\,p}(s) = g \int_{-\infty}^{c(t-T_n)} dy\, J(y)\, \alpha(t - y/c - T_n) = I_{n;\,p^-}(s) + I_{n;\,p^+}(s)$$

where

$$\begin{aligned} I_{n;\,p^-}(s) &= g \int_{-\infty}^{0} dy\, J(y)\, \alpha(t - y/c - T_n) \\ &= g \int_{s-cT_n}^{\infty} du\, J(u + cT_n - s)\, \alpha(u/c) \\ &= \frac{g}{2\sigma} \int_{s-cT_n}^{\infty} du\, e^{-(u+cT_n-s)/\sigma} e^{-u/\tau_2 c} = \frac{g\, e^{T_n/\tau_2}}{2(1 + \frac{\sigma}{\tau_2 c})}\, e^{-s/\tau_2 c}\,. \end{aligned}$$

and

$$\begin{aligned} I_{n;\,p^+}(s) &= g \int_{0}^{c(t-T_n)} dy\, J(y)\, \alpha(t - y/c - T_n) \\ &= g \int_{0}^{s-cT_n} du\, J(u + cT_n - s)\, \alpha(u/c) \end{aligned}$$

$$= \frac{g}{2\sigma}\int_0^{s-cT_n} du\, e^{(u+cT_n-s)/\sigma}\, e^{-u/\tau_2 c}$$
$$= \frac{g\, e^{T_n/\tau_2}}{2(1-\frac{\sigma}{\tau_2 c})}\, e^{-s/\tau_2 c} - \frac{g\, e^{cT_n/\sigma}}{2(1-\frac{\sigma}{\tau_2 c})}\, e^{-s/\sigma}\,.$$

Total current

$$I_{total}(s) = \sum_{n=0}^{\infty} I_n(s) = \sum_{n=0}^{N-1} I_{n;\,p}(s) + \sum_{n=N}^{\infty} I_{n;\,f}(s)$$
$$= \frac{g\left(\sum_{n=0}^{N-1} e^{T_n/\tau_2}\right)}{1-\frac{\sigma^2}{\tau_2^2 c^2}} e^{-s/\tau_2 c} - \frac{g\left(\sum_{n=0}^{N-1} e^{cT_n/\sigma}\right)}{2(1-\frac{\sigma}{\tau_2 c})} e^{-s/\sigma}$$
$$+ \frac{g\left(\sum_{n=N}^{\infty} e^{-cT_n/\sigma}\right)}{2(1+\frac{\sigma}{\tau_2 c})} e^{s/\sigma}\,. \tag{11}$$

2.2. The traveling wave solution

Once the synaptic integral $I_{syn}(\xi)$ in (9) is computed by integrating $I_{total}(s) = \sum_{n=0}^{\infty} I_n(s)$, the right hand side of expression (7) for the solution $V(\xi)$ is completely specified. The necessary condition (6) that we imposed at the beginning of our analysis now appears in the form of $I_{syn}(s)$ for $\xi \le 0$, i.e.

$$I_{syn}(\xi) = \frac{g\left(\sum_{n=0}^{\infty} e^{-cT_n/\sigma}\right)}{2(\frac{\tau_1 c}{\sigma}+1)(1+\frac{\sigma}{\tau_2 c})}\left(e^{\xi/\sigma} - e^{-\xi/\tau_1 c}\right).$$

That is, if (6) holds, then the terms $V_T e^{-\xi/\tau_1 c}$ and $I_{syn}(\xi)$ in (7) sum to $V_T e^{\xi/\sigma}$, such that $V(\xi) \to 0$ as $\xi \to -\infty$. Moreover, as we expected, the equations $V(0) = V_T$ and $V(c\,T_N^+) = \lim_{\xi \searrow c\,T_N} V(\xi) = (V_R - V_T) + V(c\,T_N) = V_R$ are valid. These results are summarized in Lemma 1 below. A more concise expression for $V(\xi)$ is provided in Theorem 1; however, we shall see that for practical purposes, Lemma 1 is very useful.

Lemma 1. *If condition (6) is true, then the following function $V(\xi)$, $\xi = tc - x$, is a traveling wave solution of the integro-differential equation (2), if all of the terms converge as ξ, $N \to \infty$.*

$$V(\xi) = V_T\, e^{\xi/\sigma}, \quad \xi \le 0\,,$$

$$V(\xi) = \left[V_T - \frac{g\left(\sum_{n=0}^{N-1} e^{-c\,T_n/\sigma}\right)}{2(\frac{\tau_1 c}{\sigma}+1)(1+\frac{\sigma}{\tau_2 c})}\right] e^{\xi/\sigma} + \frac{g\left(\sum_{n=0}^{N-1} e^{c\,T_n/\sigma}\right)}{2(\frac{\tau_1 c}{\sigma}-1)(1-\frac{\sigma}{\tau_2 c})} e^{-\xi/\sigma}$$
$$+ \frac{g\left(\sum_{n=0}^{N-1} e^{T_n/\tau_2}\right)}{(1-\frac{\sigma^2}{\tau_2^2 c^2})(1-\frac{\tau_1}{\tau_2})} e^{-\xi/\tau_2 c} - \frac{g\left(\sum_{n=0}^{N-1} e^{T_n/\tau_1}\right)}{(1-\frac{\sigma^2}{\tau_1^2 c^2})(1-\frac{\tau_1}{\tau_2})} e^{-\xi/\tau_1 c}$$
$$+ (V_R - V_T)\left(\sum_{n=0}^{N-1} e^{T_n/\tau_1}\right) e^{-\xi/\tau_1 c}, \quad c\,T_{N-1} < \xi \le c\,T_N\,(N \ge 1)\,. \tag{12}$$

Theorem 1. [general traveling wave solution] *If condition (6) is true, then the following expression for $V(\xi)$, $\xi = tc - x$, denotes a traveling solution of the integrate-and-fire model (2), if it converges:*

$$V(\xi) = \sum_{n=0}^{\infty} \eta(\xi/c - T_n) + g \sum_{n=0}^{\infty} \int_0^{\infty} J(u - \xi + c\,T_n)\, A(u/c)\, du\,. \qquad (13)$$

In (13), η is defined by (8) and A is defined as the convolution function $A(t) = \alpha * \beta\,(t) = \int_0^t \alpha(s)\,\beta(t-s)\,ds$ with $\beta(t) = \frac{1}{\tau_1}\,e^{-t/\tau_1}$, i.e.

$$A(t) = \begin{cases} 0 & , \quad t \le 0 \\ \frac{1}{1-\tau_1/\tau_2}\left(e^{-t/\tau_2} - e^{-t/\tau_1}\right), & t > 0 \end{cases}.$$

Remark 1. For any traveling wave solution with a finite number of spikes, as discussed in the next section, convergence is not an issue.

3. Solutions with a finite number of spikes

3.1. One-spike traveling waves

We focus first on the case of a solitary wave with speed c and corresponding firing time $t^*(x) = x/c$. In the notation introduced in Section 2, $T_0 = 0$ and $T_N = \infty$ for all $N \ge 1$. Therefore equation (6) reads

$$V_T = \frac{g}{2\left(\frac{\tau_1 c}{\sigma} + 1\right)\left(1 + \frac{\sigma}{\tau_2 c}\right)} \qquad (14)$$

and can be solved exactly for c, if $g/V_T \ge 2\left(1 + \sqrt{\frac{\tau_1}{\tau_2}}\right)^2$. This necessary condition for the existence of a one-spike wave was used as an existence criterion in [3,7, 16]. When this condition holds, there exist two candidate solutions, the *slow wave* and the *fast wave*, corresponding to

$$c_{\text{slow ; fast}} = \frac{\sigma}{2\tau_1}\left[\frac{g}{2V_T} - \frac{\tau_1}{\tau_2} - 1 \mp \sqrt{\left(\frac{g}{2V_T} - \frac{\tau_1}{\tau_2} - 1\right)^2 - 4\frac{\tau_1}{\tau_2}}\right].$$

As g/V_T increases from its minimal critical value to infinity, c_{slow} decreases from $\sigma/\sqrt{\tau_1\tau_2}$ to zero and c_{fast} increases from $\sigma/\sqrt{\tau_1\tau_2}$ to infinity. We will denote the curve $g/V_T = 2\left(1 + \sqrt{\frac{\tau_1}{\tau_2}}\right)^2$ as 1_F below.

In what follows, we analyze the fast one-spike traveling wave, since only this one is stable [2,7]. We will simply write c for the velocity c_{fast}.

If a traveling wave solution to (2) exists, then it takes the form $V(\xi) = V_T\, e^{\xi/\sigma}$ when $\xi \le 0$. When $\xi > 0$ it is given by, from Lemma 1,

$$V(\xi) = (V_R - V_T)\, e^{-\xi/\tau_1 c} + \frac{g\, e^{-\xi/\sigma}}{2(\frac{\tau_1 c}{\sigma} - 1)(1 - \frac{\sigma}{\tau_2 c})} + \frac{g\, e^{-\xi/\tau_2 c}}{(1 - \frac{\sigma^2}{\tau_2^2 c^2})(1 - \frac{\tau_1}{\tau_2})} - \frac{g\, e^{-\xi/\tau_1 c}}{(1 - \frac{\sigma^2}{\tau_1^2 c^2})(1 - \frac{\tau_1}{\tau_2})}.$$

Note that $\lim_{\xi \to \pm\infty} V(\xi) = 0$, $V(0) = V_T$, and $V(0^+) = V_R$.

The next step is to check that the candidate solution above indeed has no other spike after it passes $\xi = 0$; that is, the spiking threshold is never reached again. Therefore we must verify that $V(\xi) < V_T$ for all positive ξ. This is not true in general for reasons that are simple to understand. At fixed V_R, as $g/V_T \to \infty$, it becomes increasingly easier for the individual neurons to re-excite and spike again. We compute in the following the equation of a curve, call it 1_S, which separates the $(g/V_T, -V_R/V_T)$ plane to the right of 1_F into two disjoint regions: a region where the one-spike fast wave solution exists and a region where it does not.

Theorem 2. [a necessary and sufficient condition for the existence of the fast one-spike traveling wave solution] *The integrate-and-fire model (2) has a one-spike fast wave solution if and only if*

$$g/V_T \geq 2\left(1 + \sqrt{\frac{\tau_1}{\tau_2}}\right)^2 \tag{15}$$

and the reset voltage value satisfies

$$(-V_R/V_T) > (H(y^*) - 1), \tag{16}$$

where H is defined by

$$H(y) = \frac{1}{y^{\sigma/\tau_1 c}}\left[y - 1 + \frac{g/V_T}{1 - \frac{\tau_1}{\tau_2}}\left(\frac{y^{\sigma/\tau_2 c} - y}{1 - \frac{\sigma^2}{\tau_2^2 c^2}} - \frac{y^{\sigma/\tau_1 c} - y}{1 - \frac{\sigma^2}{\tau_1^2 c^2}}\right)\right] \tag{17}$$

and y^* is the unique solution in the interval $(0, 1)$ of the equation $G(y) = 0$ with

$$G(y) = y - \frac{2\tau_2 c}{\tau_2 c + \sigma}\, y^{\sigma/\tau_2 c} + \frac{\sigma(\tau_2 c - \sigma)}{(\tau_1 c + \sigma)(\tau_2 c + \sigma)}. \tag{18}$$

When (15) holds, for values of V_R for which (16) fails, there exists a positive ξ where the threshold V_T is reached again, so the one-spike condition is violated.

Proof. We sketch the proof here and provide technical details in Appendix A.

Set $y = e^{-\xi/\sigma}$. The condition $V(\xi) < V_T$ for all positive ξ reads as $V(y) < V_T$ for all $y \in (0, 1)$, which is equivalent to $H(y) < (-V_R/V_T + 1)$ with H defined by (17).

We analyze $H(y)$ and obtain that $H'(y) = \frac{\tau_2}{2\tau_1}\, \frac{\sigma}{\tau_2 c - \sigma}\, \frac{g}{V_T}\, y^{-(1+\sigma/\tau_1 c)}\, G(y)$. The sign of $H'(y)$ is the sign of $G(y)$ since for the fast wave we have $c \geq \sigma/\sqrt{\tau_1 \tau_2} > \sigma/\tau_2$.

On the interval $[0, 1]$, the function G satisfies $G(0) = \frac{\sigma(\tau_2 c-\sigma)}{(\tau_1 c+\sigma)(\tau_2 c+\sigma)} > 0$, $G(1) = -\frac{\tau_1 c(\tau_2 c-\sigma)}{(\tau_1 c+\sigma)(\tau_2 c+\sigma)} < 0$; moreover it can be proved that G has exactly one zero in this interval, say y^*. Hence, $H(y)$ has a maximum at $y = y^*$, and further, $\lim_{y\searrow 0} H(y) = -\infty$ and $H(1) = 0$. Together, these imply $H(y^*) > 0$. In summary, $V(\xi) < V_T$ for all $\xi > 0$ if and only if $(-V_R/V_T) > (H(y^*)-1)$. □

Remark 2. A special case occurs at $g/V_T = 4(1 + \tau_1/\tau_2)$, where the fast wave has the velocity $c = \sigma/\tau_1$ and

$$V(\xi) = V_T \left(-\frac{2(\tau_2+\tau_1)}{\tau_2-\tau_1} \frac{\xi}{\sigma} e^{-\xi/\sigma} + \frac{4\tau_2^2}{(\tau_2-\tau_1)^2} e^{-\tau_1\xi/\tau_2\sigma} - \frac{3\tau_2^2+2\tau_1\tau_2-\tau_1^2}{(\tau_2-\tau_1)^2} e^{-\xi/\sigma} \right) + (V_R - V_T)\, e^{-\xi/\sigma}.$$

In this case, the definition of H changes in the following way: the ratio $\frac{y^{\sigma/\tau_1 c}-y}{1-\sigma^2/\tau_1^2 c^2}$ $= -\left(\frac{y\tau_1 c}{\tau_1 c+\sigma}\right)\left(\frac{y^{\frac{\sigma}{\tau_1 c}}-1}{\frac{\sigma}{\tau_1 c}-1}\right)$ becomes $-\frac{\tau_1 c}{\tau_1 c+\sigma}\, y \ln(y)$, or equivalently $-\frac{1}{2}\, y \ln(y)$. In the computation of G, the logarithm cancels and we again end up with expression (18), i.e. y^* is again the unique solution of the equation $G(y) = 0$ on $(0, 1)$.

Remark 3. The curve 1_S which divides the plane $(g/V_T, -V_R/V_T)$ into the two regions mentioned above has the equation

$$-V_R/V_T = H(y^*) - 1\,.$$

To see that this really forms a curve in the $(g/V_T, -V_R/V_T)$ plane, note that $y^* = y^*(\sigma, \tau_1, \tau_2, c)$, with c depending on g/V_T. If we fix all parameters except g/V_T, then we get $H(y^*) = H(y^*(g/V_T))$.

Remark 4. Recall that the equation

$$g/V_T = 2\left(1 + \sqrt{\frac{\tau_1}{\tau_2}}\right)^2$$

defines the curve 1_F in the $(g/V_T, -V_R/V_T)$ plane. Theorem 2 states that to obtain a one-spike traveling wave in the integrate-and-fire model, the parameters must lie to the right of the curve 1_F for firing to occur, and above the curve 1_S for firing to stop after one spike. That is, the first condition allows for self-sustained propagation of the traveling wave, while the second prevents multiple spikings by resetting the potential to low enough values. These curves are displayed in Figure 3 for a representative parameter set.

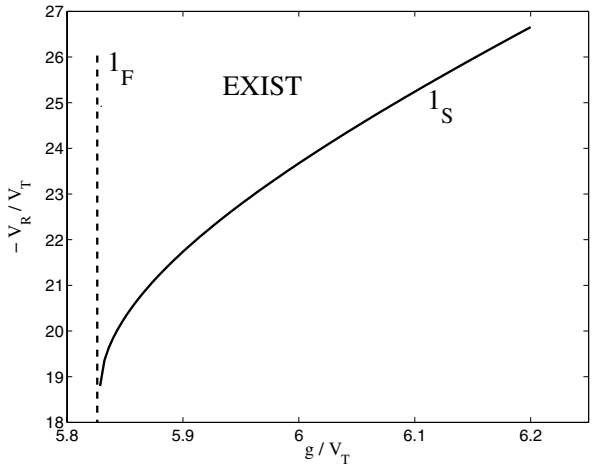

Fig. 3. The curves 1_F and 1_S for $\tau_1 = 1, \tau_2 = 2, \sigma = 1, V_T = 1$. Parameter values must lie to the right of 1_F for cells to be able to fire upon receiving the one-spike synaptic input. Parameter values must lie above 1_S for cells to stop firing after just one spike. Between the two curves, one-spike waves exist in the region labelled EXIST. Note that 1_S terminates in an intersection with 1_F, at $g/V_T = 2(1 + \sqrt{\tau_1/\tau_2})^2$ with $-V_R/V_T$ finite and positive.

3.2. Two-spike traveling waves

In a two-spike traveling wave, each cell fires at times that we denote $T_0 = 0$ and $T_1 = T$. In our earlier notation, this also means $T_j = \infty$ for each $j \geq 2$. In this case, equation (6) and substitution of the condition $V(cT) = V_T$ into (12) in Lemma 1 read as

$$V_T = \frac{g\left(1 + e^{-cT/\sigma}\right)}{2(\frac{\tau_1 c}{\sigma} + 1)(1 + \frac{\sigma}{\tau_2 c})}, \tag{19}$$

$$V_T = (V_R - V_T)\, e^{-T/\tau_1} + \frac{g}{2(\frac{\tau_1 c}{\sigma} + 1)(1 + \frac{\sigma}{\tau_2 c})} + \frac{g\, e^{-cT/\sigma}}{2(\frac{\tau_1 c}{\sigma} - 1)(1 - \frac{\sigma}{\tau_2 c})} + \frac{g\, e^{-T/\tau_2}}{(1 - \frac{\sigma^2}{\tau_2^2 c^2})(1 - \frac{\tau_1}{\tau_2})} - \frac{g\, e^{-T/\tau_1}}{(1 - \frac{\sigma^2}{\tau_1^2 c^2})(1 - \frac{\tau_1}{\tau_2})}. \tag{20}$$

With the definition

$$f(c) = \frac{2}{g/V_T}\left(\frac{\tau_1 c}{\sigma} + 1\right)\left(1 + \frac{\sigma}{\tau_2 c}\right) - 1 \tag{21}$$

we obtain according to (19) an explicit equation for T,

$$T = -\frac{\sigma}{c} \ln f(c). \tag{22}$$

We are ready now to investigate under which conditions the system (19), (20) has a solution (c, T) with positive c and T, i.e. when $f(c)$ is between 0 and 1. Let us define

$$\begin{cases} \tilde{c}_{1;2} = \frac{\sigma}{2\tau_1}\left[\frac{g}{V_T} - \frac{\tau_1}{\tau_2} - 1 \mp \sqrt{\left(\frac{g}{V_T} - \frac{\tau_1}{\tau_2} - 1\right)^2 - 4\frac{\tau_1}{\tau_2}}\right], \\ c_{1;2} = \frac{\sigma}{2\tau_1}\left[\frac{g}{2V_T} - \frac{\tau_1}{\tau_2} - 1 \mp \sqrt{\left(\frac{g}{2V_T} - \frac{\tau_1}{\tau_2} - 1\right)^2 - 4\frac{\tau_1}{\tau_2}}\right] \end{cases} \tag{23}$$

and notice that $f(c) = 0$ at $c = c_{1;2}$ and $f(c) = 1$ at $c = \tilde{c}_{1;2}$.

The set $S_c = \{\, c \in \mathbb{R}^+ \mid f(c) \in (0, 1) \,\}$ is easily computed: if $g/V_T < \left(1 + \sqrt{\frac{\tau_1}{\tau_2}}\right)^2$ then $S_c = \emptyset$; if $\left(1 + \sqrt{\frac{\tau_1}{\tau_2}}\right)^2 < g/V_T < 2\left(1 + \sqrt{\frac{\tau_1}{\tau_2}}\right)^2$ then $c_{1;2}$ are complex with nonzero imaginary parts and $S_c = (\tilde{c}_1, \tilde{c}_2)$; if $2\left(1 + \sqrt{\frac{\tau_1}{\tau_2}}\right)^2 \le g/V_T$ then $0 < \tilde{c}_1 < c_1 \le c_2 < \tilde{c}_2$ and $S_c = (\tilde{c}_1, c_1) \cup (c_2, \tilde{c}_2) \subset \mathbb{R}$.

Remark 5. $c_1 = c^1_{\text{slow}}$ and $c_2 = c^1_{\text{fast}}$; that is, c_1 and c_2 are the slow and fast velocities from the one-spike wave case. Moreover, $T(c) \to \infty$ as $c \to c_{1;2}$ since we have then $f(c) \searrow 0$.

Remark 6. As $g/V_T \to \infty$ we obtain $\tilde{c}_1, c_1 \to 0$, $c_2, \tilde{c}_2 \to \infty$ and $\tilde{c}_2/c_2 \to 2$, $\tilde{c}_1/c_1 \to 1/2$.

The equations (20) and (22) imply $F(c) = 0$, where

$$F(c) = \left(-\frac{V_R}{V_T} + 1\right) f(c)^{\frac{\sigma}{\tau_1 c} - 1} + \frac{g/V_T}{1 - \frac{\tau_1}{\tau_2}}\left(\frac{\tau_2 c}{\tau_2 c + \sigma} f_{\tau_2}(c) - \frac{\tau_1 c}{\tau_1 c + \sigma} f_{\tau_1}(c)\right), \tag{24}$$

with

$$f_{\tau_i}(c) = \begin{cases} \frac{f(c)^{\frac{\sigma}{\tau_i c} - 1} - 1}{\frac{\sigma}{\tau_i c} - 1}, & c \neq \sigma/\tau_i \\ \ln f\left(\frac{\sigma}{\tau_i}\right), & c = \sigma/\tau_i \end{cases} \qquad (i = 1, 2).$$

The velocities of candidate two-spike traveling wave solutions are precisely the roots of F that belong to the set S_c. Such velocities correspond to true two-spike traveling wave solutions if $V(\xi) < V_T$ for all $\xi > cT$.

Lemma 2. *The function $F : S_c \to \mathbb{R}$ defined by (24) is continuous on S_c and satisfies $F(\tilde{c}_1^+) = F(\tilde{c}_2^-) = -\frac{V_R}{V_T} + 1 > 0$.*

Proof. The result comes directly from the definition of F and the fact that $\lim_{c \to \tilde{c}_{1;2}} f(c) = 1$. Here and below we use the notation $F(x_0^+) = \lim_{x \searrow x_0} F(x)$, $F(x_0^-) = \lim_{x \nearrow x_0} F(x)$. □

Lemma 3. *Suppose that $g/V_T \ge 2\left(1 + \sqrt{\frac{\tau_1}{\tau_2}}\right)^2$, i.e. $S_c = (\tilde{c}_1, c_1) \cup (c_2, \tilde{c}_2)$. Then $F(c_2^+) = -\infty$ and $F(c_1^-) < 0$. Moreover*

i) *if* $2\left(1+\sqrt{\frac{\tau_1}{\tau_2}}\right)^2 \le g/V_T < 4\left(1+\frac{\tau_1}{\tau_2}\right)$, *then* $\tilde{c}_1 < \frac{\sigma}{\tau_2} < c_1 \le c_2 < \frac{\sigma}{\tau_1} < \tilde{c}_2$ *and* $F(c_1^-) = -\infty$,

ii) *if* $g/V_T = 4\left(1+\frac{\tau_1}{\tau_2}\right)$, *then* $\tilde{c}_1 < c_1 = \frac{\sigma}{\tau_2} < \frac{\sigma}{\tau_1} = c_2 < \tilde{c}_2$ *and* $F(c_1^-) = -\infty$,

iii) *if* $g/V_T > 4\left(1+\frac{\tau_1}{\tau_2}\right)$, *then* $\tilde{c}_1 < c_1 < \frac{\sigma}{\tau_2} < \frac{\sigma}{\tau_1} < c_2 < \tilde{c}_2$ *and* $F(c_1^-) = -\frac{g}{V_T}\left(1+\frac{\tau_1}{\tau_2}\right)\frac{\sigma^2}{\tau_1^2 c_1^2-\sigma^2}\frac{\tau_2^2 c_1^2}{\tau_2^2 c_1^2-\sigma^2} < 0$.

Proof. See Appendix B. □

These two lemmas immediately imply the following result. The relation between velocities described in the theorem is shown in the numerical results in Figure 4.

Theorem 3. *If* $g/V_T \ge 2\left(1+\sqrt{\frac{\tau_1}{\tau_2}}\right)^2$, *then for all* $V_R \in \mathbb{R}^-$, *there exist two distinct positive values* $c_S \in (\tilde{c}_1, c_1)$, $c_F \in (c_2, \tilde{c}_2)$ *such that* $F(c_S) = F(c_F) = 0$. *Therefore there exist two distinct solutions* (c_S, T_S), (c_F, T_F) *for the system (19), (20).*

When these correspond to two-spike traveling wave solutions, the velocity c_F *(*c_S*) of the fast (slow) two-spike traveling wave solution is greater (less) than that of the fast (slow) one-spike traveling wave solution.*

Remark 7. The above results apply for $g/V_T \ge 2(1+\sqrt{\tau_1/\tau_2})^2$. We also expect two-spike traveling waves to exist for some $g/V_T < 2(1+\sqrt{\tau_1/\tau_2})^2$, since $S_c \neq \emptyset$

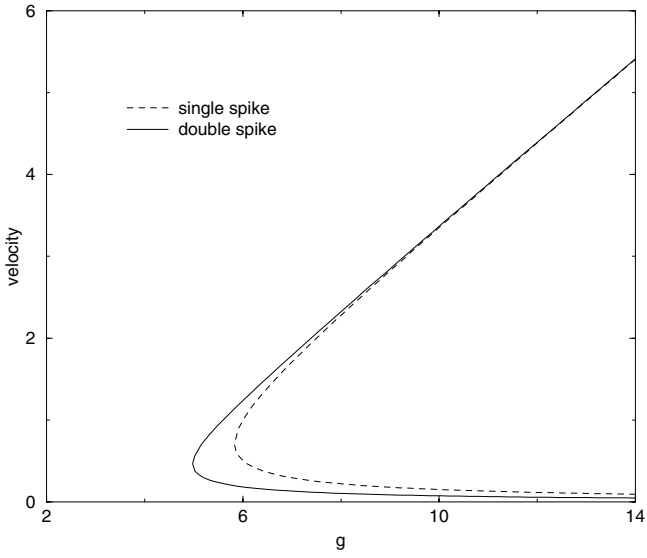

Fig. 4. Numerically generated curves showing wave speed as a function of coupling strength for one- and two-spike waves.

for $(1+\sqrt{\tau_1/\tau_2})^2 < g/V_T < 2(1+\sqrt{\tau_1/\tau_2})^2$. In fact, in analogy to the one-spike case, we expect that there exist curves 2_F, given by $g/V_T = F_2(-V_R/V_T)$, and 2_S, given by $-V_R/V_T = S_2(g/V_T)$, in the $(g/V_T, -V_R/V_T)$ plane, such that for all g/V_T to the right of 2_F, cells can fire two spikes, while for all $-V_R/V_T$ above 2_S, cells fire at most two spikes.

It is perhaps non-intuitive that, for fixed V_R and V_T, a two-spike traveling wave should exist for smaller g than needed for a one-spike wave. This holds because in a two-spike wave, the two spikes fired by each cell produce a larger overall synaptic input to each cell in the medium, which promotes firing.

We can carry these ideas further to make several reasoned conjectures. Recall that a cell's voltage is reset to V_R after a spike. For fixed V_T, as $|V_R|$ increases, a larger g is required to elicit a subsequent second spike. Hence, we expect F_2 to have a positive slope, with $F_2(-V_R/V_T) \nearrow 2(1+\sqrt{\tau_1/\tau_2})^2$ as $|V_R| \to \infty$. For fixed g and V_T, a sufficiently large value of $|V_R|$ (sufficiently strong reset) is required to prevent subsequent spikes after a second one, with a stronger reset needed for larger g. Hence, we also expect S_2 to have a positive slope. Finally, the same arguments should give corresponding curves for N-spike waves, for any positive integer N, such that N_F moves leftwards and N_S moves upwards in the $(g/V_T, -V_R/V_T)$ plane, as N increases. Figure 5 illustrates a numerically generated version of the curve 2_F, the shape of which agrees with our conjectures. The expected relation of the curves for one- and two-spike waves is drawn in Figure 6. The proofs of these conjectures remain open.

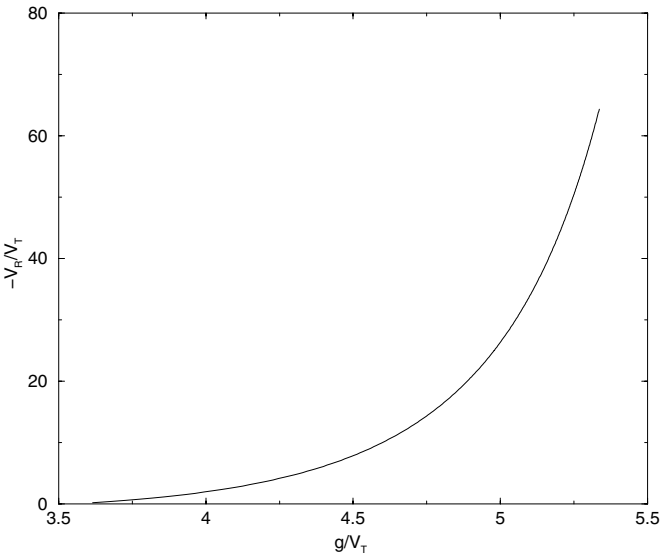

Fig. 5. Numerically generated 2_F curve. To the right of this in parameter space, cells can propagate two-spike waves.

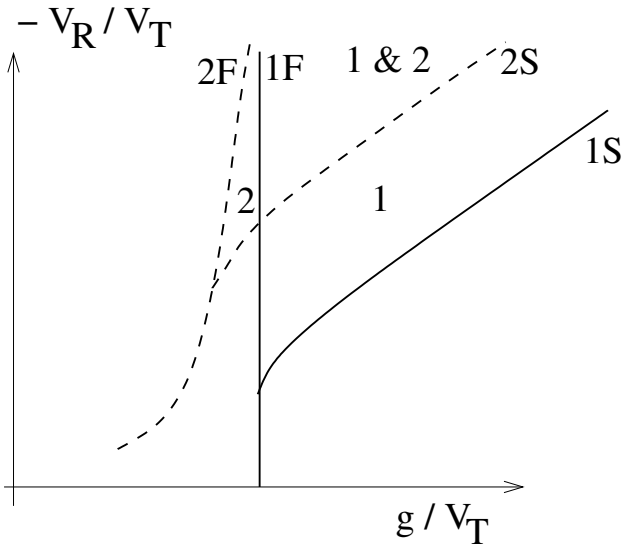

Fig. 6. Schematic illustration of the expected relation of the 1_F, 1_S, 2_F and 2_S curves in parameter space. In the regions labelled 1 or 2, one-spike or two-spike waves exist; in the region labelled 1&2, these co-exist. Outside of the labelled regions, neither type of wave exists.

By solving the equation $F(c) = 0$ numerically for fixed parameters, one can analytically find the velocity c. Given this, equation (22) yields the time T between the two spikes in the corresponding traveling wave (if it really is a two-spike solution). These results match quite closely to those obtained from numerical simulation of fast two-spike traveling waves. Numerically, waves are initiated by applying an excitatory input, or "shock," to an initial region, which leads to wave propagation away from the region [15,16]; see Figure 1. Note that wave solutions obtained in this manner are conceptually different from those studied analytically, in that the numerical waves originate at a finite time, from a specific spatial location. Thus, it is rather interesting that wave speed c and second spike time T from theory and numerics compare so well.

4. Arbitrary numbers of spikes and infinite spike trains

4.1. Computation of interspike intervals

Consider a traveling wave solution for which each cell spikes at an infinite sequence $\{x/c + T_n\}$, $n \geq 0$, of spike times. We will discuss here how the formulation given in Lemma 1 can be used to compute the interspike intervals $T_n - T_{n-1}$ between successive waves. In the traveling wave formulation, in which V is expressed as a function of $\xi = ct - x$, we have $V(cT_n) = V_T$ for each T_n. Correspondingly,

Lemma 1 implies that for any $N \geq 1$,

$$V_T = \left[V_T - \frac{g\left(\sum_{n=0}^{N-1} e^{-c\,T_n/\sigma}\right)}{2(\frac{\tau_1 c}{\sigma}+1)(1+\frac{\sigma}{\tau_2 c})} \right] e^{c\,T_N/\sigma}$$
$$+ \frac{g\left(\sum_{n=0}^{N-1} e^{c\,T_n/\sigma}\right)}{2(\frac{\tau_1 c}{\sigma}-1)(1-\frac{\sigma}{\tau_2 c})} e^{-c\,T_N/\sigma} + \frac{g\left(\sum_{n=0}^{N-1} e^{T_n/\tau_2}\right)}{(1-\frac{\sigma^2}{\tau_2^2 c^2})(1-\frac{\tau_1}{\tau_2})} e^{-T_N/\tau_2}$$
$$+ \left((V_R - V_T) - \frac{g}{(1-\frac{\sigma^2}{\tau_1^2 c^2})(1-\frac{\tau_1}{\tau_2})} \right) \left(\sum_{n=0}^{N-1} e^{T_n/\tau_1} \right) e^{-T_N/\tau_1}. \quad (25)$$

Suppose that there are a finite number of spikes in the traveling wave, say $N+1$. For each spike, equation (25) applies. In fact, one obtains a system with $N+1$ equations and $N+1$ unknowns to be solved to obtain a valid $(N+1)$-spike traveling wave solution. The unknowns are c, which denotes the velocity of the traveling wave, and the spike-times T_1 up to T_N (since $T_0 = 0$ by convention). The equations in the system are those corresponding to $V(cT_n) = V_T$, $1 \leq n \leq N$, and the equation (6). Based on the analysis in the previous section, it appears that this highly nonlinear system can only be solved numerically for most N.

The situation becomes even more complicated when an infinite number of spikes is considered. Thanks to the traveling wave description set out in Section 2, equation (25) is available, and one can iteratively solve for the spike time T_N from the previously known spike times $T_0 = 0, T_1, ..., T_{N-1}$ for every $N \geq 1$. To do so, however, an obstacle must first be overcome: since equation (6) involves all of the traveling fronts, it cannot be used independently from (25) in the case of infinitely many spikes. Thus, the velocity c that appears in each equation must be determined from some alternate source and then used here as a constant. Once c is specified from such a source, one can iteratively compute the spike times, and hence the interspike intervals $\Delta T_N = T_N - T_{N-1}$.

Remark 8. One source for the wave speed here is the fast two-spike wave speed calculated from the analytical formulas (19), (20). Numerics show that the speeds of waves with large numbers of spikes are quite similar to those calculated for two-spike waves with corresponding parameter sets. Intuitively, this makes sense because in fast two-spike waves, the interspike interval cT is significantly greater than σ, the space constant or "footprint" of the synaptic coupling; see Figures 3, 5. Even for $cT = 2\sigma$, we have $J(cT) = (1/2\sigma)e^{-2}$, such that little interaction occurs between the synaptic inputs from different waves in the same solution. Thus, waves travel with roughly the same speed, no matter how many waves there are.

One might question the value of computing the interspike intervals from numerical solution of equation (25), given that one can perform a numerical simulation of traveling waves in the full network. However, such simulations are based on applying a localized shock somewhere in the network at a fixed time and allowing waves to propagate thereafter [15, 16]. This corresponds to a different, although

closely related, form of traveling wave from that which we analyze analytically, for which all waves can be thought of as having existed somewhere in the infinite network for all time. In fact, one interesting result that arises from using equation (25) to compute interspike intervals is that we can compare theory and analysis, to see just how closely related these forms of traveling wave solutions are.

To make this comparison, we used the parameters $\tau_1 = 1$, $\tau_2 = 2$, $\sigma = 1$, $V_T = 1$, $V_R = -25$ and $g = 6$. For the first six interspike intervals, full numerical simulation of equation (2), labelled as 'Numerics,' and numerical solution of the analytical expression (25), labelled as 'Iterations,' produced excellent agreement, as shown in the following table. Note that for the analytical approach, we used $c = 1.256422$, the speed of the wave found in our numerical simulations.

	Numerics	*Iterations*	*Error*
$T1 - T0$	2.4258	2.4258	$2.83e-006$
$T2 - T1$	2.0479	2.0479	$1.56e-005$
$T3 - T2$	1.8844	1.8845	$9.72e-005$
$T4 - T3$	1.7953	1.7964	$6.22e-004$
$T5 - T4$	1.7417	1.7488	0.0040

Errors in the table grow due to difficulty in solving equation (25) numerically, resulting from the fact that the first product in this equation consists of a factor that converges to 0 as $N \to \infty$ with a factor that diverges as $N \to \infty$. Thus, we stopped after computing six interspike intervals. In full numerical simulations, the subsequent interspike intervals can be computed as well. We did this at a distance corresponding to about 40 σ away from the originally shocked region (of about 5σ), where σ is the footprint of the coupling function $J(x)$ in (4). (The total length of the domain is 100σ so that a point 40σ from the center is still far enough away from the boundary to avoid any edge effects.) We note that these intervals form a monotone decreasing sequence, which appears to converge to an asymptotic value. This will be relevant when we discuss periodic solutions in Section 4.2.

Remark 9. It can be shown, by induction on $N \geq 1$, that equation (25) is equivalent to

$$
\begin{aligned}
V_T = &\left[V_T - \frac{g\left(\sum_{n=0}^{N-1} e^{-c\,T_n/\sigma}\right)}{2(\frac{\tau_1 c}{\sigma}+1)(1+\frac{\sigma}{\tau_2 c})} \right] \cdot e^{c\,T_N/\sigma} \cdot \left[1 - e^{-(T_N - T_{N-1})(\frac{1}{\tau_1}+\frac{c}{\sigma})} \right] \\
&+ \frac{g\left(\sum_{n=0}^{N-1} e^{c\,T_n/\sigma}\right)}{2(\frac{\tau_1 c}{\sigma}-1)(1-\frac{\sigma}{\tau_2 c})} \cdot e^{-c\,T_N/\sigma} \cdot \left[1 - e^{-(T_N - T_{N-1})(\frac{1}{\tau_1}-\frac{c}{\sigma})} \right] \\
&+ \frac{g\left(\sum_{n=0}^{N-1} e^{T_n/\tau_2}\right)}{(1-\frac{\sigma^2}{\tau_2^2 c^2})(1-\frac{\tau_1}{\tau_2})} \cdot e^{-T_N/\tau_2} \cdot \left[1 - e^{-(T_N - T_{N-1})(\frac{1}{\tau_1}-\frac{1}{\tau_2})} \right] \\
&+ V_R\, e^{-(T_N - T_{N-1})/\tau_1}\,. \qquad (26)
\end{aligned}
$$

This formulation proves its advantage when we discuss the effect of adding an absolute refractory period to the integrate-and-fire model (Section 4.4).

4.2. Periodic solutions

We next analyze periodic traveling wave solutions, for which the time interval between each pair of spikes fired by any fixed neuron is a constant $T > 0$. Bressloff offers a general account of this case, but he presents his results in terms of infinite Fourier series expansions [3]. We use the formalism developed in Section 2 to obtain the dispersion relation between velocity c and period T directly. A periodic traveling wave solutions exists precisely for those values (c, T) that satisfy the dispersion relation. Our explicit calculations allow us to plot the dispersion relation, which gives insight into the range of speeds and periods for which periodic solutions can exist.

We assume that all traveling wave fronts have the same velocity c, such that they are separated by a distance cT at all times. The case of a periodic solution is different from all others we have treated, because for fixed x, we can no longer identify a first spike time $x/c + T_0$. Equation (2) must be modified accordingly, taking into account the fact that at each point in space, when we record a new spike, we assume that an infinite number of fronts have already passed and an infinite number will come. This means that the spike times should be defined as $t_n^*(x) = x/c + T_n = x/c + nT$ with $n \in \{\dots, -2, -1, 0, 1, 2, \dots\}$ and the sums in the synaptic integral and the reset term should be taken over all integers.

Under this ansatz, we analytically derive the dispersion relation, which consists of curves relating wave velocity c and time period T. To understand why periodic solutions exist for intervals of c and T values, rather than for a unique pair (c, T), note that an equation similar to (6) does not arise in the periodic case, since the assumption $\lim_{\xi\to-\infty} V(\xi) = 0$ does not apply. Suppose that a cell spikes at times 0 and T during a periodic solution. The two mathematical conditions that encode these spikes are $V(0^+) = V_R$ and $V(T) = V_T$, but, as in the previous sections, these are redundant. Therefore, the two unknowns c and T are related by only one equation.

4.2.1. Derivation of the dispersion relation

Again, we fix a point $x = 0$ as the origin for our reference frame and record, at arbitrary fixed $t \in (0, T]$, the strengths of the synaptic inputs that reach $x = 0$ from the integer-indexed sequence of traveling wave fronts in the solution. These inputs are classified as previously:

Synaptic current due to future waves Here we consider wave fronts that are at some positions $y_n \le 0$ at time t and will reach $x = 0$ in a time equal to nT, for $n \ge 1$. That is, $y_n = c(t - nT)$ and $t_n^*(x) = \frac{x}{c} + nT$, for each fixed $x \in \mathbb{R}$. The corresponding synaptic current is given by

$$\begin{aligned} I_{n;\,f}(t) &= g \int_{-\infty}^{c(t-nT)} dy\, J(y)\, \alpha(t - y/c - nT) \\ &= \frac{g}{2\sigma} \int_{-\infty}^{c(t-nT)} dy\, e^{y/\sigma}\, e^{-(t-y/c-nT)/\tau_2} \\ &= \frac{g e^{-ncT/\sigma}}{2(1 + \frac{\sigma}{\tau_2 c})}\, e^{ct/\sigma}\,, \quad n \ge 1\,. \end{aligned} \tag{27}$$

Synaptic current due to previous waves Here we consider wave fronts that are at positions $y_n > 0$ at time t. These fronts pass through $x = 0$ at times equal to $-nT$ for $n \geq 0$, such that $y_n = c(t + nT)$ and $t_n^*(x) = \frac{x}{c} - nT$ for each x for this front. The corresponding synaptic current is given by

$$I_{n;\,p}(t) = g \int_{-\infty}^{c(t+nT)} dy\, J(y)\, \alpha(t - y/c + nT) = I_{n;\,p^-}(t) + I_{n;\,p^+}(t)$$

where

$$\begin{aligned} I_{n;\,p^-}(t) &= g \int_{-\infty}^{0} dy\, J(y)\, \alpha(t - y/c + nT) \\ &= \frac{g}{2\sigma} \int_{-\infty}^{0} dy\, e^{y/\sigma} e^{-(t-y/c+nT)/\tau_2} \\ &= \frac{g e^{-nT/\tau_2}}{2(1 + \frac{\sigma}{\tau_2 c})}\, e^{-t/\tau_2}\,, \quad n \geq 0 \end{aligned} \tag{28}$$

and

$$\begin{aligned} I_{n;\,p^+}(t) &= g \int_{0}^{c(t+nT)} dy\, J(y)\, \alpha(t - y/c + nT) \\ &= \frac{g}{2\sigma} \int_{0}^{c(t+nT)} dy\, e^{-y/\sigma} e^{-(t-y/c+nT)/\tau_2} \\ &= \frac{g}{2(1 - \frac{\sigma}{\tau_2 c})} \left(e^{-nT/\tau_2} e^{-t/\tau_2} - e^{-ncT/\sigma} e^{-ct/\sigma} \right), \quad n \geq 0\,. \end{aligned} \tag{29}$$

Total synaptic current The equations (27), (28) and (29) sum to give the total synaptic current

$$\begin{aligned} I_{total}(t) &= \sum_{n=1}^{\infty} I_{n;\,f}(t) + \sum_{n=0}^{\infty} I_{n;\,p^-}(t) + \sum_{n=0}^{\infty} I_{n;\,p^+}(t) \\ &= \frac{g}{2(1 + \frac{\sigma}{\tau_2 c})} \left(\frac{e^{ct/\sigma}}{e^{cT/\sigma} - 1} \right) + \frac{g}{2(1 + \frac{\sigma}{\tau_2 c})} \left(\frac{e^{-t/\tau_2}}{1 - e^{-T/\tau_2}} \right) \\ &\quad + \frac{g}{2(1 - \frac{\sigma}{\tau_2 c})} \left(\frac{e^{-t/\tau_2}}{1 - e^{-T/\tau_2}} - \frac{e^{-ct/\sigma}}{1 - e^{-cT/\sigma}} \right) \\ &= \frac{g}{1 - \frac{\sigma^2}{\tau_2^2 c^2}} \left(\frac{e^{-t/\tau_2}}{1 - e^{-T/\tau_2}} \right) - \frac{g}{2(1 - \frac{\sigma}{\tau_2 c})} \left(\frac{e^{-ct/\sigma}}{1 - e^{-cT/\sigma}} \right) \\ &\quad + \frac{g}{2(1 + \frac{\sigma}{\tau_2 c})} \left(\frac{e^{ct/\sigma}}{e^{cT/\sigma} - 1} \right). \end{aligned} \tag{30}$$

By substituting (30) into the modified form of equation (2) and integrating over the time $t \in (0, T]$, using the condition $V(0^+) = V_R$ (or equivalently $V(T) = V_T$), we obtain the dispersion relation

$$V(c, T) = V_T \tag{31}$$

where

$$V(c,T) = V_R\, e^{-T/\tau_1} + \frac{g}{(1-\frac{\sigma^2}{\tau_2^2 c^2})(1-\frac{\tau_1}{\tau_2})}\left(\frac{e^{-T/\tau_2}-e^{-T/\tau_1}}{1-\ e^{-T/\tau_2}}\right) + \frac{g}{2(\frac{\tau_1 c}{\sigma}-1)(1-\frac{\sigma}{\tau_2 c})}\left(\frac{e^{-cT/\sigma}-e^{-T/\tau_1}}{1-\ e^{-cT/\sigma}}\right) + \frac{g}{2(\frac{\tau_1 c}{\sigma}+1)(1+\frac{\sigma}{\tau_2 c})}\left(\frac{e^{cT/\sigma}-e^{-T/\tau_1}}{e^{cT/\sigma}-1}\right). \tag{32}$$

4.2.2. Numerical computation of the dispersion relation

It is a simple matter to solve (31) numerically for a given set of parameters and thus find c as a function of T. We plot $V(c, T)$ from (32) for fixed c and $g = 6$, $\sigma = 1$, $\tau_1 = 1$, $\tau_2 = 2$, $V_T = 1$, $V_R = -25$ in Figure 7. The full dispersion relation for these parameters is shown at the left of Figure 8. Note that there are three branches of solutions to (31). This represents a significant difference from the dispersion relation for periodic solutions of the FitzHugh-Nagumo reaction-diffusion model for nerve conduction, which features two connected branches of solutions $c_f(T)$ and $c_s(T)$, joined at a minimal T value [20]. The right part of the figure shows a different view of the dispersion relation, formed by plotting the temporal frequency, $\omega = 1/T$, as a function of the wavenumber, $k = 1/(cT)$.

Heuristically, we can understand the three-branch structure of the dispersion relation in the following way. For fixed c, if T were increased from 1.6, each cell in the network would receive less and less current at each fixed time. Correspondingly,

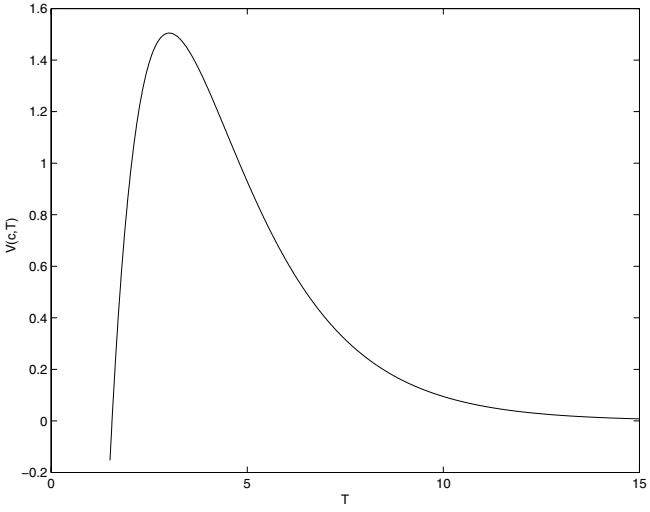

Fig. 7. V(c,T) versus T for the parameter values given in the text, with fixed $c \approx 1.25$. Points on the dispersion relation are given by intersections of $V(c, T)$ with V_T, which here has been chosen to equal 1.

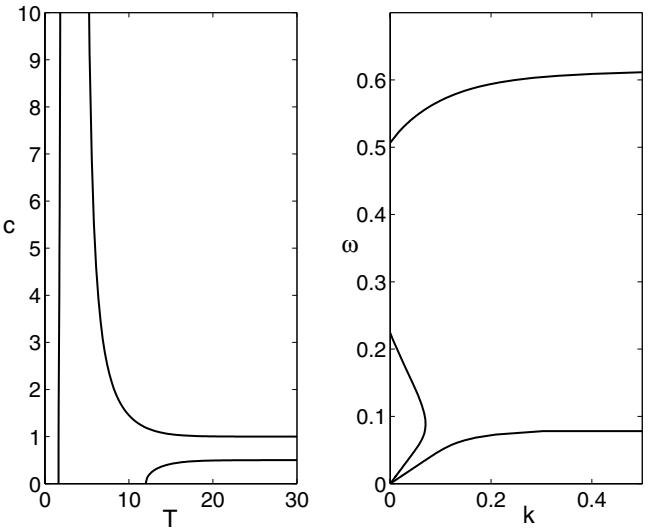

Fig. 8. The dispersion relation for $g = 6$, $\sigma = 1$, $\tau_1 = 1$, $\tau_2 = 2$, $V_T = 1$, and $V_R = -25$. Left figure: Velocity c versus period T. The left branch originates with $T \approx 1.6245$ and has a vertical asymptote at $T \approx 1.974$. The upper right branch has a vertical asymptote at $T \approx 4.464$ and a horizontal asymptote at $c = 1$. The lower right branch originates with $T \approx 11.99$ and has a horizontal asymptote at $c = 1/2$. No periodic solutions exist with periods between the two vertical asymptotes. Right figure: The same data, plotted as frequency $\omega = 1/T$ versus wave number $k = 1/(cT)$.

c must increase to deliver enough current to sustain periodic spiking. Thus, the low T branch of the relation is current-limited.

On the other hand, for very large T, spikes essentially do not interact. Thus, it is not surprising that periodic solutions can occur with approximately the speeds of the fast and slow single-spike solutions; once time T elapses after a cell spikes, the cell's voltage has recovered to approximately the right level to propagate a new single-spike wave. Consider the upper branch, corresponding to the fast wave. As T decreases from large values, if c were kept fixed, each cell would actually receive too much input to maintain a large T periodic solution. Faster speeds c are required to carry away waves that have already passed a cell, allowing the cell to recover to a state from which it can respond again. Thus, the large T, large c branch of the relation is recovery-limited. Similarly, due to the inverse relationship between speed and period that characterizes slow waves, slower speeds are needed to compensate for decreases in T, yielding the large T, small c curve.

4.3. Convergence of interspike intervals

In addition to the above heuristic interpretations of the three-branched dispersion relation, there is a natural correspondence between two of the three branches of periodic solutions given in the dispersion relation and our numerical simulations of waves, induced by a localized shock, in the full network. The low T branch of

periodics corresponds to experiments in which a single shock is applied, while for the large T - large c branch, spike interactions are limited, such that one would not expect to obtain these solutions in a single shock simulation. As an example, consider the graph of $V(c, T)$ versus T, with c fixed at approximately 1.25, the wave speed obtained from numerical simulations of the full network. This graph is presented in Figure 7.

Since $V_T = 1$, it is easy to see that the equation $V(c, T) = V_T$ has solutions at two values of T. The smaller one occurs at $T \approx 1.63612$. Recall that when we solved the integrate-and-fire equation (2) numerically, after applying a shock to an initial region, we observed that interspike intervals decayed monotonically. For example, in addition to the interspike intervals presented in the table in subsection 4.1, we find that the tenth through sixteenth interspike intervals are 1.6846, 1.6721, 1.6626, 1.6553, 1.6497, 1.6458, and 1.6437. We expect that these interspike intervals converge asymptotically towards the value of T for the (low branch) periodic solution with the same $c \approx 1.25$.

Due to the close relation between the analytically derived infinite-spike solutions considered in Section 4.1 and the solutions observed in our numerical simulations, this example suggests that two results hold, at least in certain parameter regimes. First, for fixed wave speed c, the interspike intervals of the analytically derived infinite-spike traveling waves converge in a monotone decreasing way to the low branch period of the periodic solution for that c. Second, periodic solutions are stable and are attractors for the solutions obtained in the types of numerical simulations described here.

To follow up on the first of these conjectures, for fixed $c > 0$, suppose that an infinite-spike traveling wave solution of (2) exists with spike times $\{x/c + T_n\}$, $n \geq 0$, for each x, and without loss of generality set $T_0 = 0$. We will derive a condition under which $T_1 - T_0 \equiv T_1 > T$, where T is the period of the low branch periodic solution with the same c . Henceforth, we assume $c\tau_1 > \sigma$, based on the fact that this inequality holds for c_2, the analytically computed speed of the two-spike wave.

Note the similar structures of the equation

$$V_T = V_R\, e^{-T_1/\tau_1} + g\left[\frac{\left(e^{-T_1/\tau_2} - e^{-T_1/\tau_1}\right)}{(1 - \frac{\sigma^2}{\tau_2^2 c^2})(1 - \frac{\tau_1}{\tau_2})} + \frac{\left(e^{-cT_1/\sigma} - e^{-T_1/\tau_1}\right)}{2(\frac{\tau_1 c}{\sigma} - 1)(1 - \frac{\sigma}{\tau_2 c})}\right] + \left[V_T - \frac{g}{2(\frac{\tau_1 c}{\sigma} + 1)(1 + \frac{\sigma}{\tau_2 c})}\right]\left(e^{cT_1/\sigma} - e^{-T_1/\tau_1}\right), \tag{33}$$

derived from (26) for $N = 1$ and satisfied by the infinite-spike wave, and the dispersion relation (31)–(32)

$$V_T = V_R\, e^{-T/\tau_1} + \left[\frac{g}{(1 - \frac{\sigma^2}{\tau_2^2 c^2})(1 - \frac{\tau_1}{\tau_2})}\left(\frac{e^{-T/\tau_2} - e^{-T/\tau_1}}{1 - e^{-T/\tau_2}}\right)\right.$$

$$+\frac{g}{2(\frac{\tau_1 c}{\sigma}-1)(1-\frac{\sigma}{\tau_2 c})}\left(\frac{e^{-cT/\sigma}-e^{-T/\tau_1}}{1-e^{-cT/\sigma}}\right)\Bigg] + \frac{g}{2(\frac{\tau_1 c}{\sigma}+1)(1+\frac{\sigma}{\tau_2 c})}\left(\frac{e^{cT/\sigma}-e^{-T/\tau_1}}{e^{cT/\sigma}-1}\right) \tag{34}$$

satisfied by the periodic solution.

To show that $T_1 > T$ for fixed c, it suffices to show that the right hand side of equation (33), evaluated at $T_1 = T$, is less than V_T. This will imply that at $T = T_1$, the cell at $x = 0$ in the infinite-spike wave has not yet reached V_T and fired its second spike, such that T_1 must be greater than T. Equivalently, we can show that the right hand side of equation (33), evaluated at $T_1 = T$, is less than the right hand side of equation (34).

Of course, we can neglect the first (V_R) terms, since they become identical at $T_1 = T$. Further, consider the sums in the first set of square brackets in each equation, evaluated at $T_1 = T$ for (33). For both equations, these terms are positive; however, in equation (34), each term in the sum is divided by a factor of the form $(1 - e^{-\mu})$ for a positive number μ. Hence, the sum from equation (34) is larger than that from equation (33). Thus, it suffices to show that the final term on the right hand side of equation (33), evaluated at $T_1 = T$, is less than the final term in the right hand side of equation (34).

Due to the common factors shared by these terms, this condition reduces to

$$V_T < \frac{g}{2(\frac{\tau_1 c}{\sigma}+1)(1+\frac{\sigma}{\tau_2 c})}\left(1+\frac{1}{e^{cT/\sigma}-1}\right) \tag{35}$$

Since the right hand side of (35) is nonnegative, continuous and monotonically decreasing in positive T, and blows up as $T \searrow 0$, there does exist a unique T^* such that inequality (35) holds on $(0, T^*)$. So, $T_1 - T_0 > T$ as long as $T < T^*$, or equivalently, as long as $T < (\sigma/c)\ln(H/(H-g))$ where $H = 2V_T(\tau_1 c/\sigma + 1)(1 + \sigma/\tau_2 c)$.

4.4. Absolute refractory period

After each spike, real neurons are unable to fire again during a time period called absolute refractory period. We address here the consequences of adding this feature to the integrate-and-fire model. Equation (1) is supplemented by the condition that during the refractory period, on the interval $(0, t_r)$, the potential of the neuron is held fixed at V_T. While the addition of this feature induces extra complexity in the traveling wave solutions, they retain a similar structure.

First, the interspike intervals can be computed from the following modified version of equation (26)

$$V_T = \left[V_T - \frac{g\left(\sum_{n=0}^{N-1} e^{-c\,T_n/\sigma}\right)}{2(\frac{\tau_1 c}{\sigma}+1)(1+\frac{\sigma}{\tau_2 c})}\right]\cdot e^{c\,T_N/\sigma}\cdot\left[1-e^{-(T_N-T_{N-1}-t_r)(\frac{1}{\tau_1}+\frac{c}{\sigma})}\right] + \frac{g\left(\sum_{n=0}^{N-1} e^{c\,T_n/\sigma}\right)}{2(\frac{\tau_1 c}{\sigma}-1)(1-\frac{\sigma}{\tau_2 c})}\cdot e^{-c\,T_N/\sigma}\cdot\left[1-e^{-(T_N-T_{N-1}-t_r)(\frac{1}{\tau_1}-\frac{c}{\sigma})}\right]$$

$$+\frac{g\left(\sum_{n=0}^{N-1} e^{T_n/\tau_2}\right)}{(1-\frac{\sigma^2}{\tau_2^2c^2})(1-\frac{\tau_1}{\tau_2})}\cdot e^{-T_N/\tau_2}\cdot\left[1-e^{-(T_N-T_{N-1}-t_r)(\frac{1}{\tau_1}-\frac{1}{\tau_2})}\right]$$
$$+V_R\,e^{-(T_N-T_{N-1}-t_r)/\tau_1}. \tag{36}$$

We outline here the factors that determine this new formulation. We note first that the formula for the synaptic current (30) does not change, since the refractory effects apply to the potential of the neuron and not to synaptic contributions. Second, since the cell potential is held fixed during the refractory period, it follows that the integration interval of equation (30) is reduced from $(c(T_{k-1}), cT_k)$ to $(c(T_{k-1}+t_r), cT_k)$.

Numerical simulations for $t_r = 0.3$ yield traveling waves with speed $c = 1.1871$ and the first six ISIs of 2.841, 2.517, 2.397, 2.341, 2.314, 2.3. The numerical scheme for computing ISIs can be used to compute the first three terms, 2.841, 2.520, 2.430, before numerical errors become too large.

The reduced efficiency of the ISI scheme is an effect of including the refractory period. Remember that the first term in equation (36) is the one responsible for numerical instabilities. Addition of the refractory period pushes T_N to larger values, increasing the magnitude of the factor $e^{c\,T_N/\sigma}$, which drives the numerical scheme towards instabilities faster.

Similar structural changes apply for the dispersion relationship, given in its original formulation by equations (31)–(32). When the absolute refractory period is introduced in the LIF model, equation (32) changes to

$$V(c,T) = V_R\,e^{-\frac{T-t_r}{\tau_1}} + \frac{g}{(1-\frac{\sigma^2}{\tau_2^2c^2})(1-\frac{\tau_1}{\tau_2})}\left(\frac{e^{-\frac{T-t_r}{\tau_2}}-e^{-\frac{T-t_r}{\tau_1}}}{1-e^{-T/\tau_2}}\right)e^{-\frac{t_r}{\tau_2}}$$
$$+\frac{g}{2(\frac{\tau_1 c}{\sigma}-1)(1-\frac{\sigma}{\tau_2 c})}\left(\frac{e^{-\frac{c(T-t_r)}{\sigma}}-e^{-\frac{T-t_r}{\tau_1}}}{1-e^{-cT/\sigma}}\right)e^{-\frac{ct_r}{\sigma}}$$
$$+\frac{g}{2(\frac{\tau_1 c}{\sigma}+1)(1+\frac{\sigma}{\tau_2 c})}\left(\frac{e^{\frac{c(T-t_r)}{\sigma}}-e^{-\frac{T-t_r}{\tau_1}}}{e^{cT/\sigma}-1}\right)e^{\frac{ct_r}{\sigma}}. \tag{37}$$

Numerical simulations of the full model again suggest the existence of a periodic solution, as the ISI intervals decrease monotonically towards a fixed non-zero value. The tenth such ISI has a value of 2.2858, in agreement with the value $T = 2.2845$ obtained using equation (37) with $c = 1.1871$.

The most important change in the shape of the dispersion curves, as a result of including the refractory period, is that for large enough refractory period durations t_r, the vertical asymptotes no longer exist and instead the upper branches are united, as indicated in Figure 9. However, the the existence of horizontal asymptotes is unaffected, as they correspond to solutions that approach slow and fast single-spike traveling wave solution.

We point out here how the solutions of equations (36), (37) reflect global changes induced by the refractory period on the dynamics of the traveling waves. Adding

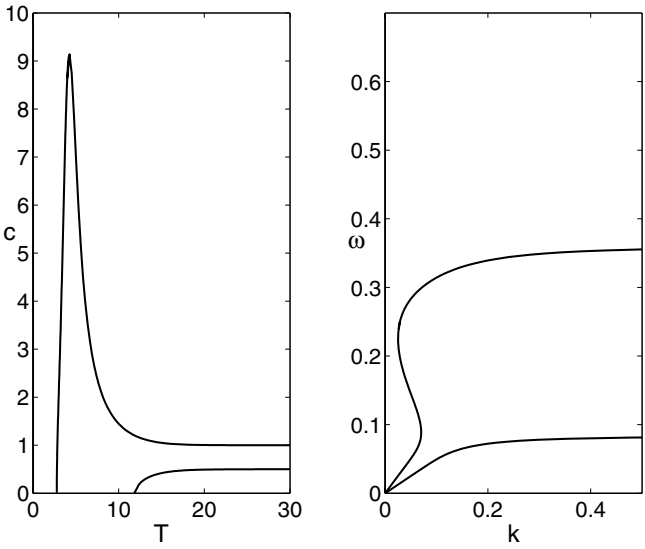

Fig. 9. The dispersion relation for $g = 6$, $\sigma = 1$, $\tau_1 = 1$, $\tau_2 = 2$, $V_T = 1$, $V_R = -25$ and $t_r = 0.6$. Left figure: Velocity c versus period T. Note that the left branch connects with the upper right branch. The newly formed branch originates with $T \approx 2.78$, has a peak at $T \approx 9.14$ and maintains its horizontal asymptote at $c = 1$. The lower right branch originates with $T \approx 11.8$ and maintains its horizontal asymptote at $c = 1/2$. Right figure: The same data, plotted as frequency $\omega = 1/T$ versus wave number $k = 1/(cT)$.

the refractory period to the model slows down wave propagation in the network due to two factors. First, holding the cell at the reset potential prevents the neuron from returning to its rest state and also limits the speed with which the cell can reach spiking threshold. Second, during the refractory period, synaptic contributions decay, thus increasing the amount of time required for the neuron to spike again. A slower wave speed ensures that when a cell emerges from refractoriness, there is still synaptic current available to push it towards threshold. Thus it is not surprising that, when comparing numerics for the $t_r = 0$ and $t_r > 0$, the latter, refractory case exhibits both a decrease in the speed of the traveling waves and an increase in the interspike intervals that separates them (at least on the small T part of the dispersion curves). Furthermore, the positive correlation between interspike intervals and refractory period also applies to periodic solutions of equation (37).

5. Summary and open problems

Traveling waves of activity are observed in slices of cortical tissue under various pharmacological manipulations [4,5,9,13,22]. These have been used both as models for epilepsy and as a way to probe the intracortical circuitry. Two of the macroscopic quantities which can be readily observed are the velocity of propagation and the number of spikes fired during a discharge (see for example, [9], where this is quantified). In previous work, [7,10,11,14,17], we studied how the velocity of traveling waves depends on various parameters by assuming that *each cell spiked once*.

In particular, conditions on the parameters which prevent propagation are readily computed. Thus, several questions remained: (i) is it possible to get multiple-spike waves; (ii) how does the existence of waves depend on having multiple spikes; (iii) how does the velocity depend on the number of spikes; and (iv) are there waves with infinitely many spikes (wave fronts)? We have attempted to address these questions in this paper by studying propagation in the integrate-and-fire model.

Lemma 1 and Theorem 1 provide two equivalent formulas for general traveling wave solutions to the continuum integrate-and-fire model (2), with the synaptic coupling functions $\alpha(t)$ and $J(x)$ given in (3) and (4), respectively. The functions defined by these formulas correspond to traveling wave solutions, for which the neuron at position x spikes at times $\{t_n^*(x) = x/c + T_n\}_{n=0}^{\infty}$, where $\xi = ct - x$, if and only if the consistency condition (6) holds and the sum $\sum_{n=0}^{\infty} e^{-cT_n/\sigma}$ converges. Convergence is not an issue, of course, when each cell fires only finitely many spikes (corresponding to $T_n = \infty$ for all but finitely many values of n). The same type of computations used to derive these formulas would be valid for other forms of $\alpha(t)$ and $J(x)$; see [14] for one example where other functions have been considered. With more complicated functions, however, difficulties in evaluating relevant integrals may arise.

We use these formulas to prove that there are curves that delineate the region on which single-spike traveling wave solutions exist, in a certain parameter space. These curves are shown in Figure 3. We also prove that in another region of parameter space, neurons can propagate a two-spike traveling wave. It remains open to determine where such solutions actually exist, by rigorously specifying the set of parameter values for which neurons stop spiking after exactly two spikes. Our reasoned conjecture on this result, illustrated in Figure 6, stems from the numerical results displayed in Figure 5. It also remains open to prove results about solutions with more than two spikes. We expect a similar pattern of regions in parameter space to extend to these cases.

The traveling wave formula in Lemma 1 is rewritten in (25), and equivalently (26) . This provides a relationship that can, in theory, be used in an iterative way to solve for as many spike times as desired in a traveling wave with any countable number of spikes, for fixed parameter values and a fixed wave speed. Numerics are needed here due to the highly nonlinear nature of (25); even with numerics, we find it difficult to compute more than about six spike times accurately in practice.

Periodic waves are different from the other cases that we treat in that in a periodic wave, these is no "first" spike time at each spatial location. Nonetheless, we are able to perform computations similar to those used to derive Lemma 1 and Theorem 1 to obtain a dispersion relation for periodic solutions in the integrate-and-fire network. By using specific coupling functions, we are able to produce a concrete analytical expression for this relation and to plot it, as done in Figure 8, although this represents a special case of a more abstract result of Bressloff [3].

Suppose that we fix a wave speed for which a periodic traveling wave solution, say of period T, exists. We expect that the time intervals between the spikes fired by any fixed cell in any other infinite-spike traveling wave solutions that exist for this speed will converge to T as the spike number increases. This result remains to be proven. In our numerical simulations, in which waves are initiated by applying

an excitation to a localized region in the network at a finite time, we observe that intervals between subsequent spikes again appear to converge. Moreover, the interspike intervals that develop appear to be a property of the medium, such that, when the wave is initiated by a localized, transient shock, the interspike intervals that arise far away from the shock are independent of the details of the shock applied. This differs from results in excitable media with diffusive coupling, as modeled, for example, by the FitzHugh-Nagumo equation; there, wave propagation appears to depend more strongly on how waves are initiated [21]. Our dispersion relation, shown in Figure 8, also differs significantly from standard excitable media results [20]. The properties of solutions generated through application of a shock, including the details of transients and the selection of a particular speed and corresponding set of interspike intervals, have not yet been investigated analytically. The latter issue in particular may relate to stability of solutions, which was not considered in this paper.

We can connect the present work with firing rate models in which spikes are completely ignored if we allow the neuron to spike continuously after shocking. There are several possible approaches. In the simplest, we suppose that the synapses saturate. Then we replace the alpha function in equation (3) by

$$\alpha(t) = 1 - \exp(-bt).$$

This means that once the neuron fires the synapse stays on for all time. Since the synapse has completely saturated and does not decay, later spikes are irrelevant and the model reduces to the "single-spike" integrate and fire model. This approximation is very good for saturating synapses which decay slowly (Ermentrout, 2003, preprint). The other way to connect this to the firing rate model is as follows. Let $A(x,t)$ denote the firing rate of the neuron at spatial point x and time t. Then

$$A(x,t) = F(I(x,t))$$

where F is the firing rate of a neuron as a function of the applied current. For the integrate-and-fire model, this is almost a threshold linear curve ([6], p. 164). Recall that the current is given by

$$I(x,t) = g \sum_{n=-\infty}^{\infty} \int_{-\infty}^{\infty} dy\, J(x-y)\, \alpha(t - t_n^*(y))$$

which can be rewritten as

$$I(x,t) = \int_{-\infty}^{t} \alpha(t-s) \int_{-\infty}^{\infty} J(x-y) \sum_n \delta(s - t_n^*(y))\, ds\, dy.$$

The sum is essentially the firing rate of the neuron ([6], p. 233), so that we obtain the closed system:

$$A(x,t) = F\left(\int_{-\infty}^{t} \int_{-\infty}^{\infty} \alpha(t-s) J(x-y) A(y,s)\, ds\, dy \right).$$

Finally, if $\alpha(t) = \exp(-t/\tau)/\tau$ we can let

$$U(x,t) = \int_{-\infty}^{t} \alpha(t-s)A(x,s)\,ds,$$

so that upon inverting the linear operator:

$$A(x,t) = \tau\frac{\partial U(x,t)}{\partial t} + U(x,t) = F\left(\int_{-\infty}^{\infty} J(x-y)U(y,t)\,dy\right).$$

This is the familiar firing rate model that has been the subject of much analysis. For smooth F such that $u = F(u)$ has three fixed points, [8] prove the existence of unique stable travelling wavefronts joining the resting state to the firing state. For the case in which $F(x) = K\max(u-u_T, 0)$ (approximating the integrate-and-fire firing rate curve) [12] also constructed travelling wavefronts. The integrate-and-fire model, by virtue of the fact that the firing rate curve is asymptotically linear is subject to runaway excitation. However, an absolute refractory period prevents this and keeps the firing rate saturated. We finally note that by adding a relative refractory process or reset to this simple firing rate model, it is possible to obtain finite spike waves since the activity will terminate once the refractoriness builds up enough.

Appendix A

Details for the proof of Theorem 2. The inequality $V(y) < V_T$ can be written as

$$\frac{g/V_T}{2(\frac{\tau_1 c}{\sigma}-1)(1-\frac{\sigma}{\tau_2 c})}\,y + \frac{g/V_T}{(1-\frac{\sigma^2}{\tau_2^2c^2})(1-\frac{\tau_1}{\tau_2})}\,y^{\sigma/\tau_2 c} - \frac{g/V_T}{(1-\frac{\sigma^2}{\tau_1^2c^2})(1-\frac{\tau_1}{\tau_2})}\,y^{\sigma/\tau_1 c}$$
$$< 1 + (-V_R/V_T + 1)\,y^{\sigma/\tau_1 c},$$

or equivalently as

$$(y-1) + \frac{2(1+\tau_1/\tau_2)}{(\frac{\tau_1 c}{\sigma}-1)(1-\frac{\sigma}{\tau_2 c})}\,y + \frac{g/V_T}{1-\frac{\tau_1}{\tau_2}}\left(\frac{\tau_2^2c^2}{\tau_2^2c^2-\sigma^2}\,y^{\sigma/\tau_2 c} - \frac{\tau_1^2c^2}{\tau_1^2c^2-\sigma^2}\,y^{\sigma/\tau_1 c}\right) < (-V_R/V_T+1)\,y^{\sigma/\tau_1 c}.$$

We used here $\frac{g/V_T}{2(\tau_1 c/\sigma-1)(1-\sigma/\tau_2 c)} - 1 = \frac{2(1+\tau_1/\tau_2)}{(\tau_1 c/\sigma-1)(1-\sigma/\tau_2 c)}$, which comes from (14).

When we regroup the terms, we obtain

$$y\left(\frac{2(1+\tau_1/\tau_2)}{(\frac{\tau_1 c}{\sigma}-1)(1-\frac{\sigma}{\tau_2 c})} - \frac{g/V_T\,(1+\tau_1/\tau_2)}{(\frac{\tau_1^2c^2}{\sigma^2}-1)(1-\frac{\sigma^2}{\tau_2^2c^2})}\right) + (y-1) + \frac{g/V_T}{1-\frac{\tau_1}{\tau_2}}\left(\frac{y^{\sigma/\tau_2 c}-y}{1-\frac{\sigma^2}{\tau_2^2c^2}} - \frac{y^{\sigma/\tau_1 c}-y}{1-\frac{\sigma^2}{\tau_1^2c^2}}\right) < (-V_R/V_T+1)\,y^{\sigma/\tau_1 c}.$$

The difference inside the first set of parentheses is zero because of (14). Therefore, we are left exactly with the inequality $H(y) < (-V_R/V_T + 1)$.

The next step is to compute the derivative of H. This is

$$H'(y) = \frac{y^{-(1+\sigma/\tau_1 c)}}{1-\frac{\tau_1}{\tau_2}} \left[\frac{\sigma(1-\frac{\tau_1}{\tau_2})}{\tau_1 c} - \left(\frac{\sigma\,(1-\frac{\tau_1}{\tau_2})\, g/V_T}{\tau_1 c} \right) \frac{\tau_2^2 c^2}{\tau_2^2 c^2 - \sigma^2}\, y^{\sigma/\tau_2 c} \right.$$
$$\left. + y \left(\frac{(\tau_1 c - \sigma)(1-\frac{\tau_1}{\tau_2})}{\tau_1 c} + g/V_T \left(\frac{\sigma^2(\frac{\tau_2^2}{\tau_1^2}-1)}{\tau_2^2 c^2 - \sigma^2} \right) \left(\frac{\tau_1 c}{\tau_1 c + \sigma} \right) \right) \right].$$

By using again equation (14) we obtain

$$H'(y) = \frac{y^{-(1+\sigma/\tau_1 c)}}{1-\frac{\tau_1}{\tau_2}} \left[\frac{\sigma(1-\frac{\tau_1}{\tau_2})}{\tau_1 c} - \frac{2(\tau_1 c+\sigma)\cdot\frac{\tau_2}{\tau_1}\cdot(1-\frac{\tau_1}{\tau_2})}{\tau_2 c - \sigma}\, y^{\sigma/\tau_2 c} \right.$$
$$\left. + y\, \frac{(\tau_1 c+\sigma)(\tau_2 c+\sigma)(1-\frac{\tau_1}{\tau_2})}{\tau_1 c(\tau_2 c-\sigma)} \right]$$
$$= \frac{(\tau_1 c+\sigma)(\tau_2 c+\sigma)}{\tau_1 c(\tau_2 c-\sigma)}\, y^{-(1+\sigma/\tau_1 c)} \left[\frac{\sigma(\tau_2 c-\sigma)}{(\tau_1 c+\sigma)(\tau_2 c+\sigma)} - \frac{2\tau_2 c}{\tau_2 c+\sigma}\, y^{\sigma/\tau_2 c} + y \right]$$
$$= \frac{\tau_2}{2\tau_1}\, \frac{\sigma}{\tau_2 c-\sigma}\, \frac{g}{V_T}\, y^{-(1+\sigma/\tau_1 c)}\, G(y)$$

with G defined by (18).

The existence of the unique root $y^* \in (0,1)$ for G comes from the following observations. Since $G'(y) = 1 - \frac{2\sigma}{\tau_2 c+\sigma}\, y^{\sigma/\tau_2 c - 1}$, the derivative of G has exactly one zero in the interval $(0,1)$, at $\tilde{y} = \left(\frac{2\sigma}{\tau_2 c+\sigma}\right)^{\tau_2 c/(\tau_2 c-\sigma)}$, G decreases on $(0,\tilde{y})$, and G increases on $(\tilde{y},1)$. Further, since we calculated that $c > \sigma/\sqrt{\tau_1\tau_2}$, the assumption $\tau_2 > \tau_1$ implies that $G(0) > 0$ and $G(1) < 0$. Therefore, $G(\tilde{y})$ must be negative, and the unique root of G belongs to $(0,\tilde{y}) \subset (0,1)$.

Appendix B

Proof for Lemma 3. The inequalities from i), ii), iii) can be easily verified. To establish the limits of F, we use these inequalities, the assumption that $\tau_2 > \tau_1$, and the fact that $\lim_{c\to c_{1;2}} f(c) = 0$.

i) By direct calculation, we obtain $\lim_{c\searrow c_2} F(c) = \lim_{c\nearrow c_1} F(c) = -\infty$.

ii) By direct calculation, we have

$$\lim_{c\nearrow c_1} F(c) = -\frac{g}{V_T}\left(1+\frac{\tau_1}{\tau_2}\right) \frac{\sigma^2}{\tau_1^2 c_1^2 - \sigma^2}\, \frac{\tau_2^2 c_1^2}{\tau_2^2 c_1^2 - \sigma^2} \quad \text{and}$$

$$\lim_{c\searrow c_2} F(c) = \lim_{c\searrow c_2} f(c)^{\frac{\sigma}{\tau_1 c}-1} \left[-V_R/V_T + 1 \right.$$
$$\left. + \frac{g/V_T}{1-\frac{\tau_1}{\tau_2}} \left(\frac{f(c)^{1-\frac{\sigma}{\tau_1 c}} - f(c)^{-\frac{\sigma}{\tau_1 c}\left(1-\frac{\tau_1}{\tau_2}\right)}}{1-\frac{\sigma^2}{\tau_2^2 c^2}} - \frac{f(c)^{1-\frac{\sigma}{\tau_1 c}}-1}{1-\frac{\sigma^2}{\tau_1^2 c^2}} \right) \right]$$
$$= -\infty\,.$$

iii) At $g/V_T = 4(1+\tau_1/\tau_2)$, since $c_1 = \frac{\sigma}{\tau_2}$ and $c_2 = \frac{\sigma}{\tau_1}$, the calculation needs to be handled more carefully. We apply l'Hospital's rule repeatedly and obtain

$$\lim_{c\searrow \frac{\sigma}{\tau_1}} f(c)^{\frac{\sigma}{\tau_1 c}-1} = 1\,,\ \lim_{c\searrow \frac{\sigma}{\tau_1}} \frac{f(c)^{\frac{\sigma}{\tau_1 c}-1}-1}{\frac{\sigma}{\tau_1 c}-1} = -\infty\,,$$

$$\lim_{c\searrow \frac{\sigma}{\tau_1}} \frac{f(c)^{1-\frac{\sigma}{\tau_2 c}}[\,f(c)^{\frac{\sigma}{\tau_1 c}-1}-1\,]}{\frac{\sigma}{\tau_1 c}-1} = 0\,,$$

and therefore

$$\begin{aligned}\lim_{c\searrow \frac{\sigma}{\tau_1}} F(c) = \lim_{c\searrow \frac{\sigma}{\tau_1}} f(c)^{\frac{\sigma}{\tau_2 c}-1}\Bigg[&(-V_R/V_T+1) f(c)^{\frac{\sigma}{\tau_1 c}\left(1-\frac{\tau_1}{\tau_2}\right)} \\ &+ \frac{g/V_T}{1-\frac{\tau_1}{\tau_2}}\left(\frac{f(c)^{1-\frac{\sigma}{\tau_2 c}}-1}{1-\frac{\sigma^2}{\tau_2^2 c^2}} - \frac{f(c)^{1-\frac{\sigma}{\tau_2 c}}\,(f(c)^{\frac{\sigma}{\tau_1 c}-1}-1)}{(1+\frac{\sigma}{\tau_1 c})(\frac{\sigma}{\tau_1 c}-1)}\right)\Bigg] \\ = -\infty\,.\end{aligned}$$

Similarly,

$$\lim_{c\nearrow \frac{\sigma}{\tau_2}} f(c)^{\frac{\sigma}{\tau_2 c}-1} = 1\,,\ \lim_{c\nearrow \frac{\sigma}{\tau_2}} \frac{f(c)^{\frac{\sigma}{\tau_2 c}-1}-1}{\frac{\sigma}{\tau_2 c}-1} = -\infty\,,\ \lim_{c\nearrow \frac{\sigma}{\tau_2}} f(c)^{\frac{\sigma}{\tau_1 c}-1} = 0\,,$$

and thus $\lim_{c\nearrow \frac{\sigma}{\tau_2}} F(c) = -\infty$. □

Acknowledgements. This work was funded by NSF grants DMS-9972913 and DMS-0108857, and by NIH grant 2R01MH47150.

References

1. Amari, S.-I.: Dynamics of pattern formation in lateral-inhibition type neural fields. Biol. Cyber. **27**, 77–87 (1977)
2. Bressloff, P.C.: Synaptically generated wave propagation in excitable neural media. Phys. Rev. Lett. **82**, 2979–2982 (1999)
3. Bressloff, P.C.: Traveling waves and pulses in a one-dimensional network of excitable integrate-and-fire neurons. J. Math. Biol. **40**, 169–198 (2000)
4. Chagnac-Amitai, Y., Connors, B.W.: Horizontal spread of synchronized activity in neocortex and its control by GABA-mediated inhibition. J. Neurophysiol. **61**, 747–758 (1989)
5. Chervin, R.D., Pierce, P.A., Connors, B.W.: Periodicity and directionality in the propagation of epileptiform discharges across neocortex. J. Neurophysiol. **60**, 1695–1713 (1988)
6. Dayan, P., Abbott, L.: Theoretical Neuroscience. MIT Press, Cambridge, MA, 2001
7. Ermentrout, G.B.: The analysis of synaptically generated traveling waves. J. Comp. Neurosci. **5**, 191–208 (1998)
8. Ermentrout, G.B., McLeod, J.B.: Existence and uniqueness of traveling waves for a neural network. Proc. Roy. Soc. Edinburgh **123A**, 461–478 (1993)

9. Golomb, D., Amitai, Y.: Propagating neuronal discharges in neocortical slices: Computational and experimental study. J. Neurophysiol. **78**, 1199–1211 (1997)
10. Golomb, D., Ermentrout, G.B.: Continuous and lurching traveling pulses in neuronal networks with delay and spatially decaying connectivity. Proc. Natl. Acad. Sci. USA **96**, 13480–13485 (1999)
11. Golomb, D., Ermentrout, G.B.: Effects of delay on the type and velocity of travelling pulses in neuronal networks with spatially decaying connectivity. Network **11**, 221–246 (2000)
12. Idiart, M.A.P., Abbott, L.F.: Propagation of excitation in neural network models. Network **4**, 285–294 (1993)
13. Kim, U., Bal., T., McCormick, D.A.: Spindle waves are propagating synchronized oscillations in the ferret LGN in vitro. J. Neurophysiol. **74**, 1301–1323 (1995)
14. Oşan, R., Rubin, J., Curtu R., Ermentrout, G.B.: Periodic traveling waves in a one-dimensional integrate-and-fire neural network. Neurocomputing **52–54**, 869–875 (2003)
15. Oşan, R., Ermentrout, G.B.: Two dimensional synaptically generated traveling waves in a theta-neuron neural network. Neurocomputing **38–40**, 789–795 (2001)
16. Oşan, R., Ermentrout, G.B.: The evolution of synaptically generated waves in one- and two-dimensional domains. Phys. D **163**, 217–235 (2002)
17. Oşan, R., Rubin, J., Ermentrout, G.B.: Regular traveling waves in a one-dimensional network of theta neurons. SIAM J. Appl. Math. **62**, 1197–1221 (2002)
18. Pinto, D.J., Ermentrout, G.B.: Spatially structured activity in synaptically coupled neuronal networks: I. Traveling fronts and pulses. SIAM J. Appl. Math. **62**, 206–225 (2001)
19. Pinto, D.: Personal communication
20. Rinzel, J., Keller, J.B.: Traveling wave solutions of a nerve conduction equation. Biophys. J. **13**, 1313–1337 (1973)
21. Stich, M.: Target patterns and pacemakers in reaction-diffusion systems. Ph.D. Dissertation, Technical University Berlin, 2002
22. Traub, R.D., Jefferys, J.G.R., Miles, R.: Analysis of propagation of disinhibition-induced after-discharges along the guinea-pig hippocampal slice in vitro. J. Physiol. Lond. **472**, 267–287 (1993)